AD-A153 509 STUDIES ON SURFACE PROCESSES DURING FRICTION AND WEAR (U) VIRGINIA UNIV CHARLOTTESVILLE SCHOOL OF ENGINEERING AND APPLIED SCIENCE D KUHLMANN-WILSDORF MAR 85 1/1

UNCLASSIFIED N00014-83-K-0245 F/G 20/11 NL

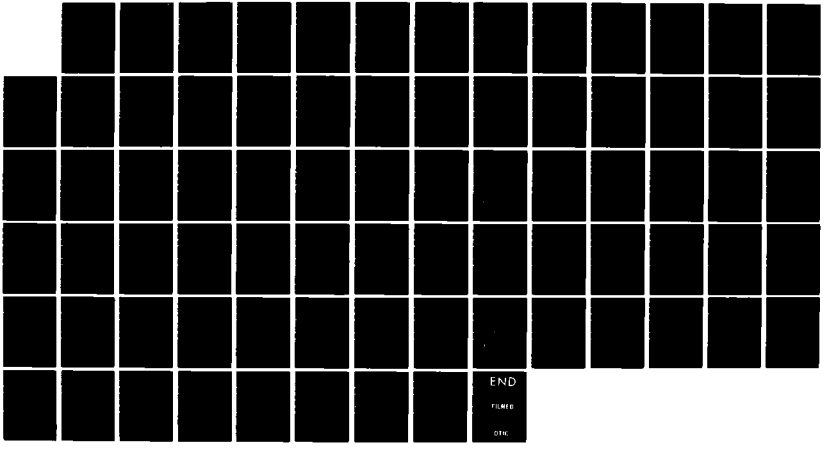

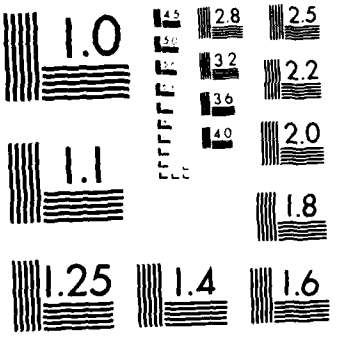

MICROCOPY RESOLUTION TEST CHART
NATIONAL BUREAU OF STANDARDS 1963 A

AD-A153 509

End of Year Report

STUDIES ON SURFACE PROCESSES DURING FRICTION AND WEAR

Sponsored by:

OFFICE OF NAVAL RESEARCH

Materials Division (Tribology)

800 N. Quincy Street
Arlington, Virginia, 22217
Attention: A. W. Ruff

Submitted by:

Doris Kuhlmann-Wilsdorf
University Professor of Applied Science

CONTRACT No. N00014-83-K-0245
March 1985

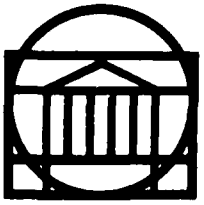

SCHOOL OF ENGINEERING AND APPLIED SCIENCE

DTIC ELECTE MAY 08 1985

UNIVERSITY OF VIRGINIA

CHARLOTTESVILLE, VIRGINIA 22901

DTIC FILE COPY

85 03 07 170

Accession For
NTIS GRA&I
DTIC TAB
Unannounced
Justification
By
Distribution/
Availability Codes
Dist
A-1

End of Year Report

STUDIES ON SURFACE PROCESSES DURING FRICTION AND WEAR

Submitted to:

Materials Division (Tribology)
Attention: A. W. Ruff
Office of Naval Research
Contract No. N00014-83-K-0245

by

Doris Kuhlmann-Wilsdorf
University Professor of Applied Science
Department of Materials Science
University of Virginia
Charlottesville, VA 22901

In the previous contract period, experimental as well as theoretical research has been carried out. The former has concentrated on the development of a novel testing apparatus which promises to reveal hitherto inaccessible details on the surface condition of materials during sliding. It employs simultaneous measurements of the coefficient of friction and the electrical contact resistance, using a "soft" set-up and following the momentary variations. This research has not yet yielded reportable results but progress is most encouraging.

Theoretical work has been devoted to theory of plastic deformation, and a review on workhardening theory has been written due to be published in Trans. Met. Soc. While this is progressively leading to a deeper understanding of metal plasticity, and in this much is valuable, no particularly noteworthy new results have emerged.

Of by far the greater interest in connection with the present contract theme, namely friction and wear and surface processes governing these, has been the research embodied in the two extensive papers which are appended herewith. As is seen from these, it has been possible to derive rather simple analytical, closed equations for the evaluation of the momentary temperature at contact spots during sliding. This theory has been extended to the case of concurrent friction and Joule heating, as presented in the third, shorter enclosed paper, which has been submitted to the WEAR OF MATERIALS - 1985 conference.

Submitted to WEAR
(mailing date 8/25/1985)

DE-MYSTIFYING FLASH TEMPERATURES - II APPLICATION TO HEATING THROUGH FRICTION AT PLASTICALLY DEFORMED CONTACT SPOTS

by

D. Kuhlmann-Wilsdorf
Department of Materials Science
University of Virginia, Charlottesville, VA 22901

Abstract

In Part I expressions for the flash temperatures at elliptical contact spots, ΔT_e, were derived. They were uniformly found to be proportional to q, the rate of heat evolution per unit area of contact. In the case of frictional heat, q is proportional to the velocity of sliding, v, and also depends on the total force, P, exerted between the two relatively sliding objects and the number, N, of contact spots at which they touch. For plastically deformed contact spots (which is by far the most frequent case) the following expressions are found, using the listed symbols. For the characteristic velocity $v_o = \kappa_1\sqrt{\pi N H_s}/\sqrt{P} = p/\sqrt{P}$; for the flash temperature in general

$$\Delta T_e = (\mu\sqrt{PH_s/\pi N}\ v/\lambda_1)/(1/Z_o S+\lambda_r/S_o) = (\mu H_s v_r/c_1\rho_1)/(1/Z_o S+\lambda_r S_o)$$

where $Z_o(v_r\lesssim 2) = 1/(1+v_r/3)$, $Z_o(v_r\gtrsim 2) = (9/8)/(\sqrt{v_r} + 1/\sqrt{8})$,

$S(v_r\lesssim 1) \simeq S_o = (4/3/\sqrt{(1+e^{3/4}/3)(1+1/3e^{3/4})}$ and

$$S(v_r\gtrsim 1) = (e^{1/4}+e^{1/4}/\sqrt{8v_r})/(1+e^{3/4}/\sqrt{8v_r});$$

for the flash temperature at very low speeds for circular contact spots

$$\Delta T_o(v_r<<1) = \mu\sqrt{PH_s/\pi N}\ v/(\lambda_1+\lambda_2) = j\mu\sqrt{P}\ v;$$

for the flash temperature at very high speeds for circular contact spots

$$\Delta T_o(v_r>>1) = (9\mu/8\lambda_1)(\kappa_1^2 H_s^3 P/\pi N)^{1/4}\ \sqrt{v} = g\mu P^{1/4}\ \sqrt{v};$$

and for the flash temperature of circular contact spots at $v_r=1$,

$$\Delta T_o(v_r=1) = (\mu H_s/\rho_1 c_1)/(4/3+\lambda_r) = b\mu \ .$$

The model is expanded to include that in actual fact the heat is evolved in a narrow zone in the softer material just below the contact spot. For that case a maximum attainable temperature (if below the melting point) is found, of roughly

$\Delta T_{max} = \mu(10\pi/3)H_s/\rho_s c_s = f\mu$, attained at a speed in the order of $100v_o$.

In order to assist in the practical application of the above equations, tables are presented of approximate values of the parameters p, j, g, b and f for a number of metals and three non-metals. Pin/disk asymmetries arise because at high speeds the heat flow is practically independent of the pin material but is determined by the substrate, unless it is a very poor heat conductor compared to the pin.

Lastly, in case that the contact spot moves relative to both sides, with speeds v_1 and v_2, i.e. relative velocities $v_{r1} = \kappa_1 R$ and $v_{r2} = \kappa_2/R$ where $R = \sqrt{F/\pi}$, it is, in general,

$$\Delta T_e = (\mu\sqrt{PH_s/\pi N}\ v/\lambda_1)/[1/Z_o(v_{r1})S(v_{r1}) + \lambda_r/Z_o(v_{r2})S_{(v_{r2})}].$$

List of Symbols

a	Radius of circular contact spots
b	Parameter for the computation of $\Delta T_o(v_r = 1)$
B	Workhardening coefficient
c	Specific heat
e	Ratio of axes in the direction of sliding and at right angles thereto of elliptical contact spots
f	Parameter for the computation of ΔT_{max}
F	Area of contact spot
g	Parameter for the computation of $\Delta T_o(v_r \gg 1)$
H_s	Hardness of the softer side
j	Parameter for the computation of $\Delta T_o(v_r \ll 1)$
L	Sliding distance
m	Width of the deforming zone on the soft side in units of a
n	Measure of the thickness of the deforming zone on the soft side
N	Number of contact spots
p	Parameter for the computation of v_o
$\overline{p}$	Average normal pressure at contact spots (equal to H_s in case of plastically deformed contact spots).
P	Normal force between two sliding solids
P_N	Normal force at single contact spot
P_T	Tangential force at single contact spot
q	Heat input per unit area and unit time at contact spots
$R = \sqrt{F/\pi}$	Characteristic dimension of contact spots
S	Shape factor for elliptical spots in relative motion
S_o	Shape factor for elliptical contact spots at rest
$\delta t = a/v_o$	Characteristic time interval

T_M	Melting temperature
ΔT_o	Flash temperature of circular contact spot at v_r-value indicated, or else for $v = v_o$
$\Delta T_{ch} = \mu H_s/\rho_1 c_1$	Characteristic temperature
ΔT_e	Flash temperature of elliptical contact spots
ΔT_h	Flash temperature at high speeds
ΔT_ℓ	Flash temperature at low speeds
ΔT_{max}	Maximum temperature within the deformed zone of the soft side
v	Velocity
v_{crit}	Speed at which in the high-speed approximation ΔT_{max} would be reached
$v_o = \kappa/R$	Characteristic velocity
$v_r = v/v_o$	Relative velocity
V	Heated volume
W_{in}	Mechanical energy input into one contact spot
$\dot{W}_{in}$	Rate of energy input to one contact spot
$Y = v_r Z_o$	Function used by Jaeger (2) to express the velocity dependence of flash temperatures in case of friction heat.
Z_o	Function used to compute the velocity dependence of flash temperatures of circular contact spots
Z_{ho}	Z_o at high speeds
$Z_{\ell o}$	Z_o at low speeds
z	Coordinate normal to the interface
z_o	Depth below contact spot on the softer side at which shear is at maximum
δz	Depth to which the heat diffusion front has penetrated into the substrate

γ	Subsurface shear strain on the soft side
γ_s	Subsurface shear strain at z_o
κ	Heat diffusivity
μ	Coefficient of friction
τ	Subsurface shear stress on the softer side
τ_o	Critical resolved shear stress of the softer material at small shear strains
τ_s	Subsurface shear stress on the softer side at depth z_o

Subscripts

1	Referring to substrate
2	Referring to asperity side
N	Referring to number of contact spots
o	Referring to circular spots, except for v_o which is applicable also to elliptical spots.

De-Mystifying Flash Temperatures - II Application to Heating Through Friction at Plastically Deformed Contact Spots

by

D. Kuhlmann-Wilsdorf
Department of Materials Science
University of Virginia, Charlottesville, VA 22901

Introduction

In part I the basic equations for the flash temperatures, ΔT, of elliptical contact spots were derived. Invariably ΔT was found to be proportional to q, the rate of heat input per unit area of contact spot. When heating is due to friction, q is proportional to the velocity. Specifically, for a contact spot of characteristic radius R and ellipticity e = A/B, with A and B the axes in, and at right angles to, the direction of sliding, respectively, we have in accordance with Fig. 1, with $R = \sqrt{AB}$, and P_N the normal force

$$q = \mu P_N v/\pi R^2 = \mu \bar{p} v \ , \qquad (1a)$$

where $\bar{p}$ is the average normal pressure over the contact area.

The value of $\bar{p}$ depends on conditions. When P_N is gradually raised from zero pressure, $\bar{p}$ increases until it reaches the Meyer hardness, H, (see ref. 1). Within a fairly narrow margin that pressure is then maintained until the contact spots have spread to the point that they occupy a sizeable fraction of the macroscopic contacting area and they begin to interact. In the typical sliding situation the actual contact area is much smaller than the macroscopic area of contact and, conversely, the normal forces exerted are large enough to cause local plastic deformation at the contact spots of the softer side. In these cases, then,

$$q = \mu H_s v \qquad (1b)$$

with μ the coefficient of friction and v the sliding speed. The otherwise

redundant subscript s is used here as a reminder that H_s is the hardness of the softer side, whether it be the asperity or substrate side.

In the following we shall examine the flash temperatures arising in this condition of plastically deformed contact spots, with particular emphasis on unlubricated "adhesive" wear between metals.

The Basic Equations

a) Circular Contact Spots

Fur unlubricated "adhesive" wear with plastically deformed contact spots, the relative motion between the two sides is accomodated through subsurface shear in the softer side according to Fig. 2. We shall defer discussion of the consequences of the fact that the heat is developed within either the asperity side or the substrate side, and shall for the time being revert to the model of Fig. 1 in which the heat is evolved in the interface. We may then write for the flash temperature of a circular contact spot of radius $a = \sqrt{F/\pi} = R$ and area F, in accordance with eq. 1 of Part I,

$$\Delta T_o = \mu H_s R v/(\lambda_1/Z_o+\lambda_2), \tag{2}$$

where the symbols are mostly the same as in part I. Specifically, λ is the thermal conductivity and Z_o is a function of relative velocity, v_r,

$$v_r = v/v_o = v/(\kappa_1/R) \tag{3}$$

where

$$v_o = (\kappa_1/R) = \lambda_1/\rho_1 c_1 R\ . \tag{4}$$

Here κ_1 is the thermal diffusivity, ρ_1 is the mechanical density, and c_1 is the specific heat of the substrate side, - meaning the side relative to which the contact spot moves, while it is stationary on the asperity side.

As was shown in part I,

$$Z_o(v_r \leq 2) \cong Z_{\ell o} = 1/(1+v_r/3) \tag{5a}$$

and

$$Z_o(v_r \gtrsim 2) \cong Z_{ho} = (9/8)/(\sqrt{v_r}+1/\sqrt{8}) \tag{5b}$$

which for quite large values of v_r reduces to

$$Z_o(v_r >> 1) = 9/8\sqrt{v_r} \ . \tag{5c}$$

Introducing the relative thermal conductivity of the asperity side as

$$\lambda_r = \lambda_2/\lambda_1, \tag{6}$$

the characteristic temperature rise as

$$\Delta T_{ch} = \mu H_s R v_o/\lambda_1 = \mu H_s/\rho_1 c_1, \tag{7}$$

and the function

$$Y = v_r Z_o, \tag{8}$$

as used by Jaeger (2), we can rewrite eq. 2 into the more convenient form

$$\Delta T_o = \Delta T_{ch}/(1/Y+\lambda_r/v_r) = \Delta T_{ch} v_r/(1/Z_o+\lambda_r). \tag{9a}$$

Fig. 3 shows $\Delta T_o/\Delta T_{ch}$ as a function of λ_r and v_r, using Z_o according to Jaeger's computation (Fig. 7 of ref. 2) as reproduced in Fig. 2 of Part I. As seen, for small speeds, when $Z_o=1$, $\Delta T_o/\Delta T_{ch}$ rises linearly, namely as

$$(\Delta T_o/\Delta T_{ch})_{v<<v_o} = v_r/(1+\lambda_r) \tag{9b}$$

and at intermediate and high speeds when eq. 5b applies,

$$(\Delta T_o/\Delta T_{ch})_{v \gtrsim 2v_o} = v_r/[(8/9)(\sqrt{v_r}+1/\sqrt{8})+\lambda_r] \tag{9c}$$

in accordance with the corresponding expressions for Z_o (eqs. 5b and 5c).

b) Elliptical Contact Spots

For elliptical contact spots the appropriate expression for the flash temperature is, corresponding to eq. 35 of Part I,

$$\Delta T_e/\Delta T_{ch} = 1/(1/YS+\lambda_r/S_o v_r) = v_r/(1/Z_o S+\lambda_r/S_o) \ . \tag{10}$$

The shape factor S was derived in Part I. For $v_r \gtrsim 1$ it is

$$S(v_r \gtrsim 1) = (e^{1/4}+e^{1/4}/\sqrt{8v_r})/(1+e^{3/4}/\sqrt{8v_r}) \tag{11}$$

and for $v_r \lesssim 1$ it is

$$S(v_r \lesssim 1) \cong S_o = (4/3)\sqrt{(1+e^{3/4}/3)(1+1/3e^{3/4})} \quad . \tag{12}$$

Correspondingly, for velocities below v_o, S_o appears in eq. 10 not only in conjunction with λ_r but also with Z_o so that

$$(\Delta T_e/\Delta T_{ch})_{v_r \lesssim 1} \cong S_o v_r/(1/Z_o+\lambda_r) \; . \tag{13}$$

In fact, except for the introduction of $\Delta T_{ch} = \mu H_s/\rho_1 c_1$ in lieu of $q\sqrt{F/\pi}/\lambda_1$, and multiplication with v_r this is eq. 34 of Part I. Figs. 4 to 6 show $\Delta T_e/\Delta T_{ch}$ for the same choice of parameters for which $\Delta T_o/(q\sqrt{F/\pi}/\lambda_1)$ was computed and represented in Figs 7-9 of Part I.

Application to "Adhesive" Sliding

a) The Model

While Fig. 1 is an oversimplification of the actual, vastly more complicated case of frictional heating at contact spots between sliding solids, Fig. 2 is still an idealization, although rather more realistic. It envisages that the mechanical work input

$$W_{in} = \mu P \tag{14}$$

when two solids slide past each other for unit distance under the normal force P is totally converted into heat via plastic deformation. Indeed, the fraction of W_{in} which is stored in the form of crystal defects is typically very small (e.g. ref. 3) and it may well be overbalanced by additional heating through chemical reactions at the surface such as through oxidation.

In agreement with a previously developed model (4,5), it is assumed that the shearing takes place in the softer material underneath the contact spots and is essentially confined to a zone ma wide and a/n thick where

$2<m\lesssim 4$ and $2\lesssim n\lesssim 50$ with $m\approx 3$ and $n\approx 10$ good average values.

Since according to this model the shearing zone typically is much thicker than incidental surface films, their presence will not greatly affect the results. However, it has already been noted that, strictly speaking, the heat evolution does not take place at the interface, where indeed there will normally be relative rest and thus no heat evolution of any significance at all, but within the softer side quite close to the interface.

This concept is akin to the proposal of Rozeanu and Pnueli (6,7) that shear instabilities could concentrate the relative displacement into a narrow subsurface region which becomes strongly heated. Yet, the present model has a different physical basis, since there is always enforced relative rest at the interface on account of micro interlocking to a relief depth of, say, z_o on average, where $z_o \lesssim 1000\text{Å}$ (ref. 4). For the remainder at depths $z>z_o$ the shear stress appears (4,8), to drop as

$$\tau = \tau_s z_o/\frac{1}{2}(z+z_o), \tag{15}$$

While a representative work hardening law, linking subsurface shear, γ, to the prevailing stress, τ, is (4)

$$\tau = \tau_o + B \ln \gamma . \tag{16}$$

Consequently, after repeated passes, or a sufficiently long sliding distance that quasi-equilibrium is established, we expect

$$\gamma = \gamma_s \exp\{\tau_s(z_o-z)/B(z_o+z)\} \tag{17}$$

with

$$\gamma_s = \exp\{(\tau_s-\tau_o)/B\} . \tag{18}$$

Previously, (4) values for τ_o, τ_s and B were semi-quantitatively inferred from published measurements of $\gamma(z)$ for a worn copper pin (9) and were found to be compatible with the known materials properties and sliding

TABLE II

	Ag	Al	Au	Be	Cr	Cu	Fe	Ir	Mg	Mo	Ni	Pb	Pd	Pt	Sn	Ta	Ti	W	Zn	Brass	Steel	Glass	Brick	Granite
Ag	4.3	4.8	5.2	7.0	8.2	5.0	8.3	8.5	4.4	7.1	8.2	2.8	8.2	8.2	2.7	8.5	9.2	6.7	7.2	8.5	8.5	9.5	9.5	9.5
Al		7.2	5.8	8.4	11.0	5.1	11.3	11.7	6.8	8.7	10.8	5.2	10.8	10.8	4.7	11.5	13.4	7.8	9.5	11.7	11.7	14.4	14.4	14.3
Au			6.1	8.2	10.0	5.5	10.2	10.5	5.4	10.8	10.0	3.7	9.9	9.9	3.5	10.4	11.6	7.7	9.0	10.5	10.5	12.2	12.2	12.1
Be				23.0	26.0	7.9	20.8	34.5	8.2	23.8	29.3	6.8	21.4	19.9	6.0	30.3	35.4	20.9	14.5	26.8	34.5	33.4	45.8	45.5
Cr					42.1	9.3	34.4	48.2	11.2	27.3	41.2	12.4	34.4	31.9	9.9	46 6	67.2	22.8	21.3	45.7	48.2	74.0	83.2	82.1
Cu						5.5	9.5	9.7	4.7	8.0	9.3	3.0	9.3	9.3	2.9	9.6	10.5	7.5	7.7	9.7	9.7	11.0	11.0	11.0
Fe							36.4	39.7	11.5	21.8	33.6	13.3	33.6	33.6	10.4	38.3	56.8	18.2	22.1	39.7	39.7	71.4	71.9	70.8
Ir								92.7	12.1	39.8	54.6	14.8	39.3	36.4	11.3	59.4	88.3	39.6	23.5	53.5	84.5	98.5	222	179
Mg									7.9	8.4	11.0	6.5	11.0	11.0	5.8	11.8	14.3	7.4	9.3	12.1	12.1	15.8	15.8	15.7
Mo										27.0	31.2	7.2	22.4	20.8	6.3	31.9	37 7	23.7	15.1	28.2	39.8	35.7	53.8	53.4
Ni											46.8	12.0	33.7	31.2	9.7	52.9	75,3	26.2	20.9	44.6	54.6	70.9	92.6	91.4
Pb												18.0	12.0	12.0	12.7	14.2	24.3	5.9	8.6	14.8	14.8	34.8	35.2	34.4
Pd													33.7	31.2	9.7	38.1	54.3	18.9	20.9	39.3	39.3	66.3	66.7	65.8
Pt														31.2	9.7	35.2	50.2	17.4	20.9	36.4	36.4	61.3	61.7	60.9
Sn															10.1	11.9	16.0	5.3	7.4	11.3	11.3	19.8	19.9	19.7
Ta																57.2	83.3	26.4	22.9	51.5	59.4	91.4	113	111
Ti																	174	30.0	29.6	79.9	88.3	277	332	316
W																		25.3	13.0	23.3	39.6	27.8	50.3	50.1
Zn																			17.0	23.5	23.5	33.7	33.9	33.5
Brass																				53.5	53.5	98.5	105	103
Steel																					84.6	98.5	166	164
Glass																						2100	2520	1740
Brick																							7050	2020
Granite																								2870

MATERIAL	$\rho/10^3$	c	λ	$\kappa/10^{-4}$	$H/10^8$	P_{10}	B*	G_{10}	F*	T_M
Ag	10.5	233	418	1.71	3 - 7	21	88	50	2100	960°C
Al	2.7	880	210	0.86	1.4-4	8.2	52	47	1300	660
Au	19.3	129	310	1.18	2 - 7	14.0	77	51	1900	1063
Be	1.85	1750	150	0.46	15	10.0	200	160	4900	1280
Cr	7.1	440	67	2.17	7-13	3.8	140	186	3400	1903
Cu	8.9	381	380	1.14	4 - 7	15	70	48	1700	1083
Fe	7.8	452	60	0.17	6	2.3	73	125	1800	1539
Ir	22.4	134	50	0.167	27	4.9	380	460	9400	2443
Mg	1.74	1005	159	0.91	2	7.2	49	48	1200	657
Mo	10.0	250	140	0.56	18	13	310	222	7500	2610
Ni	8.8	446	70	0.178	7 - 20	3.7	150	200	3600	1453
Pb	11.3	126	35	0.25	0.5	1.0	15	40	370	327
Pd	12.2	247	70	0.25	4 - 10	3.6	100	143	2500	1552
Pt	21.4	132	70	0.25	4 - 8	3.4	91	130	2200	1772
Sn	7.3	223	64	0.38	.45-.6	1.5	14	28	337	232
Ta	16.6	138	54	0.24	12	4.7	220	280	5500	2996
Ti	4.5	611	17	0.062	11	1.2	170	420	4200	1668
W	19.3	134	180	0.70	12 - 40	20	430	250	10,500	3380
Zn	7.1	384	111	0.41	3 - 6	4.9	71	85	1700	420
Brass	8.5	377	50	0.33	9	5.6	120	230	2900	
Steel	7.8	490	50	0.12	15 - 30	3.2	250	340	6200	
Glass	2.4	840	1.2	.0058	8	0.09	170	1400	4200	
Brick	2.6	840	0.8	.0038	40(?)	0.13	780	5800	19,000	
Granite	2.4	960	1.7	0.012	30	0.37	560	3900	14,000	

TABLE I

References

1) E. Holm, R. Holm and E.I. Shobert, J. Appl. Phys., 20 (1949) 319; compare also R. Holm, Electric Contacts (Fourth Edition) Springer Berlin/ New York 1967, pp. 372-375.

2) J.C. Jaeger, Proc. Roy. Soc. N.S.W., 56 (1942) 203.

3) A.L. Titchener and M.B. Bever , Progress in Metal Physics, Pergamon, New York, Vol. 7 (1958) 247.

4) D. Kuhlmann-Wilsdorf, in "Fundamentals of Friction and Wear of Materials", Ed. D.A. Rigney, Am. Soc. Metals, Metals Park, OH, (1981) p. 119.

5) D. Kuhlmann-Wilsdorf, in "Wear of Materials- 1983", Ed. K.C. Ludema, Am. Soc. Mech. Eng., New York (1983) p. 402.

6) L. Rozeanu and D. Pnueli, J. Lubrication Technology, ASME, 100 (1978) 4; 479.

7) D. Pnueli and L. Rozeanu, in Rept. Thermomechanical Effects Workshop Dartmouth, June 19/20, 1984; to be published in Wear.

8) D. Kuhlmann-Wilsdorf and L.K, Ives, Wear 85 (1983) 359.

9) J.H. Dautzenberg and J.H. Zaat, Wear 23 (1973) 9.

10) R.A. Burton (Ed.) Thermal Deformation in Frictionally Heated Systems, Elsevier Sequoia, Lausanne/New York, 1980; see also Wear 59 (1980) pp. 1-290.

by a factor of 3 for Ni/Ti, of ∿10 for steel/granite, and ∿6 for Mg/Cu. The values in Table III suggest that flintlock ignition is theoretically the best, indeed the only realistically feasible, manner to generate a spark in one strike.

13) Pb and Sn are much softer than engineering materials. Hence these deform when paired with those, and the flash temperatures are correspondingly low. Thus Pb and Sn platings provide fine lubrication layers.

14) Hard platings by contrast can transfer the shear strain to the other side that may be less sensitive or less used, e.g. from pin to disk. Also, hard platings will mostly reduce μ and thus the flash temperatures.

15) The theory may be readily expanded to the case in which the contact spot moves relative to both sides, as may occur in gears. In that case, in terms of the contact velocities v_1 and v_2 relative to the two sides, with $v = v_1 + v_2$, it is $v_{r1} = \kappa_1/R$, $v_{r2} = \kappa_2/R$ and

$$\Delta T_e/(\mu\sqrt{PH_s/\pi N}\, v) = 1/[\lambda_1/Z_o(v_{r1})S(v_{r1}) + \lambda_2/Z_o(v_{r2})S(v_{r2})] \ .$$

Acknowlegements

The financial support of this research through the Materials Division (Tribology) of the Office of Naval Research, Arlington, VA, is gratefully acknowledged.

coefficient of friction, - in actual fact thus on the shear strength of the softer material.

7) The data in Table 1 yield this maximum temperature to be above the melting point if the coefficient of friction lies above $\sim 1/2$, on average. However, in fact the melting temperature of the softer side cannot be much exceeded because the material loses its shear strength and thus the coefficient of friction drops strongly

8) The critical velocity at which the maximum temperature is reached is estimated at about 100 v_o or moderately less.

9) Again, using characteristic values of the parameters involved, v_o is found as low as $\sim$1m/sec at P=1N for lead, and as high as $\sim$20m/sec for silver and for tungsten. Since v_o is proportional to $1/\sqrt{P}$, it can be as low as 1cm/sec for railroad wheels.

10) The flash temperature at $v=v_o$ is independent of P, but is proportional to μ. For $\mu \simeq 1/3$ it ranges between $\sim$5°C for Sn and 140°C for W.

11) For low speeds, $\Delta T_o = j \mu \sqrt{P}\, v$ where j depends on both of the materials. For Sn/Pb, for example, $j \simeq 13$ and for Ag/Sn it is $j \simeq 3$ in mks units. However, j is quite high for hard materials and those with low thermal diffusivities, (e.g. it is $j \cong 90$ for titanium on iridium).

12) In the high-speed regime, pin/disk asymmetries arise. These can be further accentuated because geometry and heat flow favor long-lived deforming asperities on the pin and therefore the pin tends to assume the role of the soft material even if ordinarily it would be the harder one. Therefore, while the disk controls the heat flow, the pin typically controls the heat generation. A table of estimated values shows that on reversal of pin/disk roles for the same materials, the temperature rise at the interface can differ by a factor of several; specifically

lubricants. Conversely, Ti tends to run "hot" among the metals, both on account at high hardness and of low heat conductivity.

The by far lower heat conductivities of ceramics as compared to metals, finally, cause flash temperatures of these to be very much higher, to which their generally greater hardness still adds. Interestingly, according to table III, trial and error led to the best choice for making fire in striking flint against steel in flintlock rifles.

Summary

1) Flash temperatures cannot be given accurately because, in nature, they are ill-defined and vary greatly from place to place and moment to moment.
2) Even so, good estimates are possible, provided essential parameters are known.
3) Speeds are slow or fast relative to a characteristic speed v_o. At that speed the "diffusion distance" of the heat energy equals the characteristic dimension of the contact, a, within the time δt during which the substrate moves through the length of its radius - more or less. I.e. in the interval $dt \cong a/v_o$ the diffusion distance is, $\delta_z = \sqrt{\kappa \delta t} = a$, while the spot moves through $a = \sqrt{\kappa a/v_o}$.
4) Significantly below v_o, the asperity acts much as if it were at rest, and the heat flows into the two materials in proportion to their heat conductivities, λ_1 and λ_2.
5) At high speeds, and provided that $v_r >> \lambda_r^2$, the softer material heats adiabatically through rapid shear at the interface, but the heat flows practically exclusively into the substrate, so that only its heat conductivity enters into the problem.
6) In the fully adiabatic case, when shearing takes place only in the softer material, a maximum temperature is reached which depends on the size of the shear zone relative to the size of the contact spot and on the

answers presented in this paper are upper limits as far as the discussed shift of the zone of heat evolution is concerned.

b) Reliability of Results

It will have become clear that the critical parameter in calculations of flash temperatures is v_o since it is in comparison to this velocity that actual velocities must be judged as "slow" or "fast". Fortunately, v_o depends on the root of both the number of contact spots and hardness, so that errors in these parameters do not affect the result sensitively. However, as seen in table I, for same P and N, the characteristic velocity v_o has very widely different values depending on the material, while it decreases with increasing P, and increases when N increases.

If the input parameters are all known, eq. 10 in conjunction with eqs. 5a and 5b for the determination of Z_o, and eqs. 11 and 12 for S and S_o, respectively, will give results within a few percent of the accurate mathematical solution for model I. This is amply satisfactory and no further refinements appear to be worthwhile on account of the unavoidably larger errors and uncertainties which arise due to discrepancies between the model and actuality, e.g. as in Fig. 2 and through erratic changes in N and spot shape. Further, a more thorough study will have to include the changes of λ, ρ, κ, c and H_s with temperature. Fortunately, with the exception of H_s, these are minor.

c) Qualitative Features of Results

Notwithstanding the above limitations, the results obtained are very helpful. Clearly, for example, under otherwise same conditions materials run "hot" or "cool" principally depending on their thermal conductivity and hardness. Thus, as evident from Tables I to III, Pb and Sn always run "cool" on account of their very low hardness, and thus they may be used as effective

Lastly Table III demonstrates the pin/disk asymmetry for a number of material pairings, assuming for the pin either one half of the listed hardness, or the lowest value in the range of H_s listed for the pin material. No values of j are given if those pin hardnesses lie above the upper hardness value given for the substrate, on the assumption that in such a case the substrate material will continue to slide. As already indicated, pin/disk asymmetry will be also expected in that case, but the corresponding values can be readily calculated and might confuse the reader if they were also included in Table III.

Discussion

a) Effect of Sub-Surface Instead of Interfacial Heat Evolution

The above graphs (Figs. 3 to 6) and Tables I to III should go far to aid experimentalists in making rapid estimates and/or calculations of the flash temperatures due to friction in unlubricated adhesive sliding. With some caution these may be also used in the presence of minor surface films, but not necessarily if sliding is not "adhesive". The deciding factor is whether the heat is evolved at restricted contact spots sufficiently small and sufficiently widely separated that the models of Fig. 1 or 2 are applicable.

As to the displacement of the zone of heat evolution somewhat into the interior of the softer material, this will have the lesser effect, the more closely to the surface it is situated. At any rate, the highest temperatures will be in the softer material and the heat flow into the harder side will be diminished. Correspondingly, also, the surface itself will be at a lower temperature than calculated on the basis of the model in Fig. 1.

By and large it appears, intuitively, that the above effects will not be major, and for this reason the theory has been presented making use of the model in Fig. 1, and the contact spot size has been used rather than the somewhat larger area of actual heat evolution. Future investigations will have to determine the magnitude of the consequent error. At any rate, it would seem that the

Further, in computing p_{10}, b*, g_{10} and f* in table I, the average value of H was used where a range rather than a single value was given. At any rate, hardnesses vary widely from specimen to specimen, as also with temperature, and therefore all of the values given for the computed parameters are guide-line values only, and certainly not accurate. The use of those parameters is in accordance with eqs. 22, 25, 26 and 29 namely, for circular spots,

(i) Find v_o, the characteristic velocity for the listed material on the substrate side, as

$$v_o = p_{10}/\sqrt{P} \tag{33}$$

(ii) Find the flash temperature for the material sliding on itself with speed v_o as

$$\Delta T_o(v_r=1) = \mu b^* \tag{34}$$

(iii) Find the flash temperature in the case of $\sqrt{v_r} >> \lambda_r$, and the listed material as the substrate, as

$$\Delta T_o(v_r >> \lambda_r^2) = g_{10}\mu^4\sqrt{P}\,\sqrt{v} \tag{35}$$

(iv) Find the estimated maximum temperature in the listed material when it acts as the softer side as

$$\Delta T_{max} = f\mu \tag{36}$$

provided that $\Delta T_{max} < T_M$, since otherwise melting inhibits further rise of energy input. Note, therefore, that the ratio $\Delta T_{max}/f$ provides an estimate of the lowest coefficient of friction which can lead to melting.

In table II are listed values of j according to eq. 24. With their aid the flash temperatures at low speed (i.e. $v_r \leq 1$) may be found as

$$\Delta T_o(v_r \leq 1) = \mu\sqrt{P}\, v\, j\ . \tag{37}$$

Since low speeds are concerned here, there is no pin/disk asymmetry. Again the average values of H_s are chosen, extracted from Table I.

exists for the simple reason that on reversal of the two materials λ_r changes from, say, 1/2 to 2, or 4 to 1/4, etc. As seen from Fig. 3 this causes the corresponding, typically quite marked change of flash temperatures. To the extent that wear rates go up with temperature this means that making the pin of the more highly heat conducting material will generally decrease the wear rate.

It may be added here that the time intervals in which contact spots are stationary on the substrate side need be no longer than 2a/v or $\sqrt{eF/\pi}/v$, respectively, to make the equations applicable. If the spot moves in regard to <u>both</u> sides, the appropriate values of Z_o and S must be applied also in connection with λ_r in all of the above equations.

Numerical Examples

The experimentalist is often interested in some rough estimates but not interested to go through the equations in detail. In such cases the curves in Figs. 3-6 should be very helpful. To simplify the task even more, Tables I to III present some approximate values for the hardness and the parameters p (eq. 22b), j (eq. 24b), b (eq. 25b), g (eq. 26b) and f (eq. 29b).

Specifically, in Table I are collected the values for ρ, c, λ, κ, H, p, b, g, f and the melting temperatures for a number of materials, - in regard to specific conditions which are explained in the legend to Table I, where also the significance and use of those parameters is more fully explained.

Throughout, N = 10, m = 3, and n = 10 have been assumed. It is, of course, a simple task to convert to other values of N, m and n; e.g. indicating the chosen value of N, the number of contact spots, by the corresponding subscript (as done in Table I), we have

$$P_N = P_{10}\sqrt{N/10}, \tag{32}$$

and similarly in regard to m and n whose reasonable ranges are believed to be $2 \leq m \leq 4$ and $4 \leq n \leq 50$ while $1 \leq N \leq 100$.

Pin-Disk Asymmetries

The above expressions for v_{crit}/v_o and $\Delta T_{max}/\Delta T_o(v_r=1)$ are somewhat cumbersome on account of the factor $\rho_l c_l/\rho_s c_s$. This reduces to unity if the substrate is the softer material but otherwise can lie within a rather wide range of values depending on the materials concerned. At any rate, v_{crit}/v_o will almost certainly be much larger than unity so that the high speed approximation for Z_o applies, unless λ_r is rather large (see Fig. 3) in which case eq. 2 or 10 in conjunction with eq. 5b must be applied.

At first glance it may appear strange that the "substrate" side might be the softer side just as well as the "asperity" side, for the reason that one intuitively tends to think of the asperity as being sheared. However, on which side the contact is stationary, whether for short or extended periods, is not so much a question of materials properties than of macroscopic geometry: If one of the two members is much smaller than the other, such as in a pin and disk or block and ring arrangement, contact spots can be stationary only on the smaller object, i.e. the pin or disk, but not on the larger one.

A stationary contact spot tends to bulge out through thermal expansion, which increases the load. This then causes further expansion in the typical thermo-mechanical behavior (compare ref. 10). Further, the bulk temperature of the smaller member, i.e. normally the asperity side, will tend to rise more and, lastly, as already discussed, the heat is not strictly speaking generated in the interface but on the softer side. All of these effects have the tendency to favor sliding in the smaller member, i.e. the pin, and thus cause its wear, even if normally its material should be the harder.

This, then, is a cause of strong pin/disk asymmetry. However, even if the discussed reversal in the role of the "softer" material does not occur on reversal of pin and disk materials, yet a significant pin/disk asymmetry

the width of which is controlled geometrically. Let us then ask what the maximum temperature is which may be attained in that zone. To this end we proceed much as in deriving the equations in Part I, as follows:

The energy input when a contact spot moves through distance L is

$$W_{in} = \mu(P/N)L = \mu\pi a^2 H_s L \tag{27}$$

which is expended in the volume

$$V = ma(a/n)L \tag{28}$$

according to Fig. 2. Provided that the velocity is high enough so that the heating in that volume is essentially adiabatic, the resulting temperature rise is

$$\Delta T_{max} = W_{in}/\rho_s c_s V = \mu\pi H_s n/\rho_s c_s m = f\mu \tag{29a}$$

with

$$f = \pi H_s n/\rho_s c_s m \tag{29b}$$

where the subscript s reminds us that the softer material is concerned.

Comparing eq. 29 with eqs. 22, 25 and 26 shows that the above maximum temperature would be reached in the high-speed case at the critical speed v_{crit} given by

$$v_{crit}/v_o = [(8\pi n/9m)(\rho_1 c_1/\rho_s c_s)]^2 \tag{30}$$

and that ΔT_{max} relates to $\Delta T(v_r = 1)$ as

$$\Delta T_{max}/\Delta T_o(v_r = 1) = (\pi n/m)(4/3+\lambda_2/\lambda_1)(\rho_1 c_1/\rho_s c_s) \quad . \tag{31}$$

Physically, the significance of ΔT_{max} is this: Provided that the values of ΔT computed according to eqs. 23 or 26a lie well below ΔT_{max}, they are presumed to be rather reliable and the heatflow to be well described by the model of Fig. 1. However, as the computed values approach ΔT_{max}, they have to be regarded with skepticism and are in all likelihood too large.

$$v_o = \kappa_1\sqrt{\pi N H_s}/\sqrt{P}=p/\sqrt{P} \tag{22a}$$

with

$$p = \kappa_1\sqrt{\pi N H_s} \tag{22b}$$

and the flash temperatures for circular contact spots (eqs. 2 and 9) are found as

$$\Delta T_o = \mu\sqrt{P H_s/\pi N}v/\lambda_1(1/Z_o+\lambda_r) \tag{23}$$

in general. At very low speeds eq. 23 reduces to

$$\Delta T_{\rho o}= \mu\sqrt{P H_s/\pi N}v/(\lambda_1+\lambda_2) = j\mu\sqrt{P}\ v \tag{24a}$$

with

$$j = \sqrt{H_s/\pi N}\ /(\lambda_1+\lambda_2)\ , \tag{24b}$$

while at the characteristic speed of v_o it is

$$\Delta T_o(v_r=1) = (\mu H_s/\rho_1 c_1)/(4/3 + \lambda_r) = b\mu \tag{25a}$$

with

$$b = (H_s/\rho_1 c_1)/(4/3+\lambda_r), \tag{25b}$$

and at high speeds such that $\sqrt{v_r}>>\lambda_r$ and $v_r\gtrsim 2$, at the least,

$$\Delta T_o(v_r>>1) = \Delta T_h = (9\mu/8\lambda_1)\sqrt{v}(\kappa_1^2 H_s^3 P/\pi N)^{1/4} = g\mu P^{1/4}\sqrt{v} \tag{26a}$$

with

$$g = (9/8\lambda_1)(\kappa_1^2 H_s^3/\pi N)^{1/4}\ . \tag{26b}$$

The Maximum Attainable Temperature

Eq. 26 can clearly not apply to any arbitrarily high velocity. The most obvious limit to the flash temperature is the melting point of either of the two sides. Once this is attained, the coefficient of friction must drop precipitously (ice-skating being the best-known example) and thereby the work-input.

According to Rozeanu and Pruely (6, 7) melting can occur through a thermo-mechanical instability. This may well be possible. However, as was discussed above in connection with Fig. 2, one must expect the heat generation not to occur at the interface in any event, but within a narrow zone

conditions. The expended mechanical energy density found from 15 to 18 is, for $z>z_o$

$$\tau\gamma = \tau_s\gamma_s[2z_o/(z_o+z)]\exp\{(\tau_s/B)(z_o-z)/(z_o+z)\}. \qquad (19)$$

Since invariably (τ_s/B) will be larger than unity and more typically be in the order of 10, the decrease of energy density input with depth described by eq. 19 is very rapid. E.g. for $\tau_s/B = 10$ it decreases by a factor of 40 between $z = z_o$ and $z = 2z_o$.

Thus the zone of heat evolution will be very narrow and hence be well approximated by a mathematical plane as in Fig. 1 for the great majority of cases. That, even so, the parameter n appearing in Fig. 2 is not estimated to be larger than 50 and more typically is believed to be about 10, is for reasons of geometry, in that contact spots cannot be expected to be accurately Planar over their whole extent but will be warped. Indeed, one may feel rather comfortable with the estimate of n = 10, being confident that it will mostly be good to within a factor of less than two.

b) The Parameters q and a (or R)

Overwhelmingly, the softer side is plastically deformed and its compression hardness, H_s, determines the total contacting area under total normal load P. Therefore, if there are N contact spots, assumed to be circular, their radius is found as

$$a = \sqrt{P/\pi N H_s}\ . \qquad (20)$$

If now, over the total contact area $N\pi a^2$, the frictional work is dissipated at the rate $\dot{W}_{in} = \mu P v$, the power density q becomes

$$q = \dot{W}_{in}/N\pi a^2 = \mu H_s v \qquad (21)$$

(see eq. 1b).

With this, the characteristic velocity (eq. 4) is found as

TABLE III

DISK \ PIN	AG	AL	BE	CU	MG	NI	TI	ZN	BRASS	STEEL	GRANITE
AG	34	23	67	42	15	64	54	34	46	---	---
AL	48	33	--	60	21	91	76	48	65	---	---
BE	49	33	97	61	22	93	77	49	67	164	164
CU	30	21	60	38	13	58	48	31	41	---	---
MG	65	44	127	81	29	123	103	65	88	---	---
NI	66	45	130	81	29	124	103	66	89	219	---
TI	160	108	315	197	70	300	250	160	216	530	---
ZN	63	43	124	78	28	118	99	63	85	---	---
BRASS	125	85	247	155	55	236	197	125	170	---	---
STEEL	75	51	149	93	33	142	119	75	100	251	251
GRANITE	700	476	1400	870	307	1300	1100	700	950	2300	2300

Legends

Fig. 1 Idealized model of contact spot.

Fig. 2 More realistic model of contact spot seen in cross section at right angles to the direction of motion, including micro-roughness deformed zone.

Fig. 3 Theoretical flash temperatures for circular contact spots according to eq. 9 as a function of velocity and relative heat conductivity, λ_r.

Fig. 4 Theoretical flash temperatures for elliptical contact spots with ellipticities as indicated as a function of velocity according to eqs. 10 to 12 for $\lambda_r=0$.

Fig. 5 As Fig. 4 but for $\lambda_r=1$.

Fig. 6 As Fig. 4 but for $\lambda_r=10$.

Table 1:

Approximate values, in mks units throughout, of density (ρ), specific heat (c), thermal conductivity (λ), thermal diffusivity (κ), hardness (H), and melting temperature (T_M) for a number of materials, together with the parameters p_{10} (i.e. p of eq. 22b for the case of N = 10 and the material serving as substrate), b* (i.e. b of eq. 25b for the case of the two sides being of the same material), g_{10} (i.e. g of eq. 26b for the case of N = 10, and the material serving as substrate and being the softer member), and f* (i.e. f of eq. 29b for the case that the listed material serves as the softer member, that n = 10, and that m = 3).

The values of those parameters and their use (for circular contact spots under the named conditions and choosing the average value of H where a range is given) are as follows:

$$p_{10} = \kappa\sqrt{10\pi H}\ ; \qquad v_o = p/\sqrt{P}$$

$$b^* = (H/\rho c)/(4/3 + 1)\ ; \qquad \Delta T_o(v_r \ll 1) = \mu b$$

$$g_{10} = (9/8\lambda)(\kappa^2 H^3/10\pi)^{1/4}\ ; \qquad \Delta T_o(v_r \gg 1) = g\mu P^{1/4}\sqrt{v}$$

$$f^* = 10\pi H/3\rho c\ ; \qquad \Delta T_{max} = f\mu$$

Thus p_{10} gives an indication of the characteristic speed. E.g. under otherwise same conditions, v_o is roughly 20 times larger for silver than for lead, and 200 times larger than for glass.

Further, g_{10} gives a qualitative impression whether the respective materials tend to "run" hot or cool at high relative speeds. Namely, large values indicate relatively high flash temperatures, i.e. hot contact spots, and low values cool contact spots. Hence, tin runs coolest (and therefore is a good lubricant plating) while the non-metals run hot.

Next f* is useful in judging (roughly) whether a material is liable to melt, or undergo some phase change etc., through friction, since $\mu = \Delta T_{max}/f$ is the lowest coefficient of friction at which some specific temperature ΔT_{max} (e.g.

that at which austenite transforms to martensite) can be reached.

Lastly, b^* is a guide to the flash temperature that is to be expected at intermediate speeds for any given value of μ.

Note that ΔT is proportional to the coefficient of friction in all cases. Hence the most obvious corrective measure in order to decrease flash temperatures would be to decrease μ, e.g. through lubrication.

Table II

Values of $j_{10} = \sqrt{H_s/\pi N}/(\lambda_1 + \lambda_2)$ according to eq. 24, for N = 10, based on the values in Table I, assuming the average value of H where a range is given. From these find the temperature rise for circular contact spots at low speeds; - for $v_r \leq 0.7$ with an error of less than 20%, for $v_r \leq 3$ within better than a factor of two, and in each case obtaining an upper limit. Namely, $\Delta T_{\ell o} = j\mu\sqrt{P}\ v$. Since under otherwise same sliding conditions the flash temperature is proportional to j, as seen, it is evident how much hotter the contact spots are for non-metal on non-metal than when at least one metal is involved. Note the consistently low values of j when at least one of the sliding member is a very good heat conductor, e.g. Ag, Al, Au, Cu and Mg, while values involving Sn are low principally on account of its low hardness.

Table III

Selected g_{10} values as in Table I with N = 10, but (i) choosing H_s as either one half of the H value given in Table I, or as the lower value if a range was indicated, and (ii) only if with that choice the pin will serve as the softer material as compared to the average or upper hardness listed for the disk material in Table I. When even so the disk material is found to be softer the corresponding box is left blank. Note the very pronounced changes of flash temperature expected on interchanging pin and disk, by comparing paired values along diagional lines from bottom left to top right. For example, g_{10} changes from 13 for a magnesium pin sliding on a copper disk to 81 for a copper pin on a magnesium disk. Hence the occasionally considerable changes in wear rates on such interchanges become understandable. Significantly, the highest value of all arises for a steel pin on a granite (flint) substrate. Thus the choice of materials in flintlock rifles was most apt and, according to this table, perhaps the only feasible one

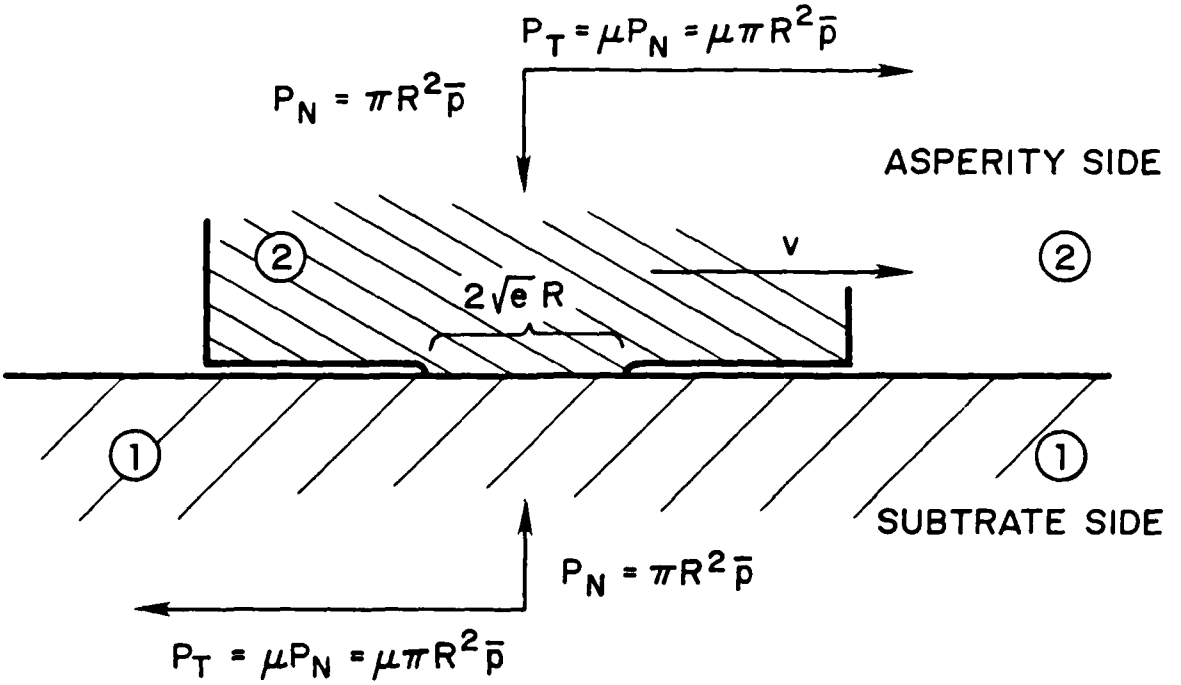
$P_T = \mu P_N = \mu \pi R^2 \bar{p}$
$P_N = \pi R^2 \bar{p}$
ASPERITY SIDE
2
v
2
$2\sqrt{e}\,R$
1
1
SUBTRATE SIDE
$P_N = \pi R^2 \bar{p}$
$P_T = \mu P_N = \mu \pi R^2 \bar{p}$

Part II Fig. 1

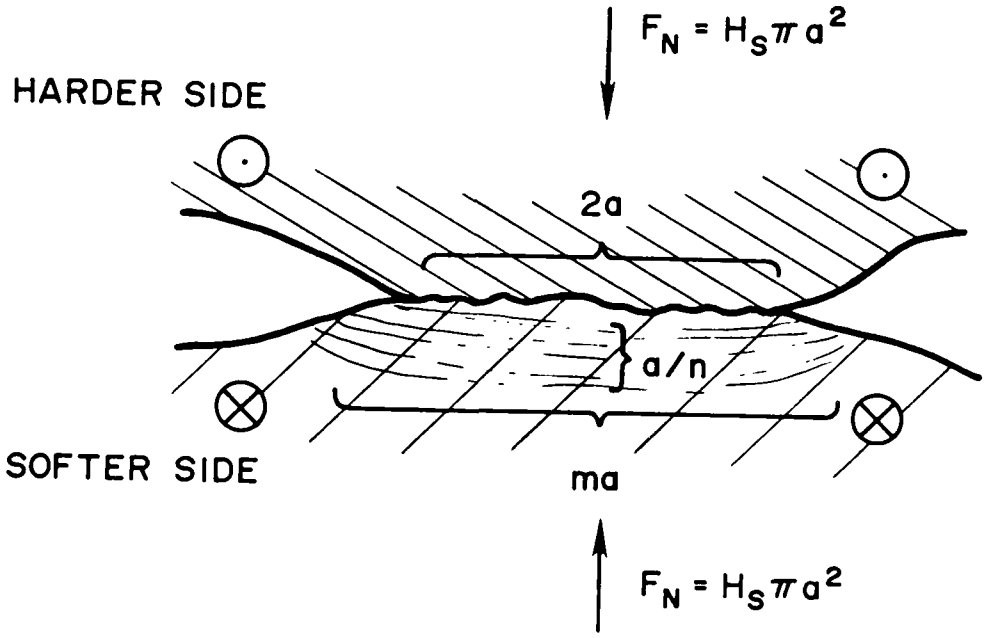

Part II Fig. 2

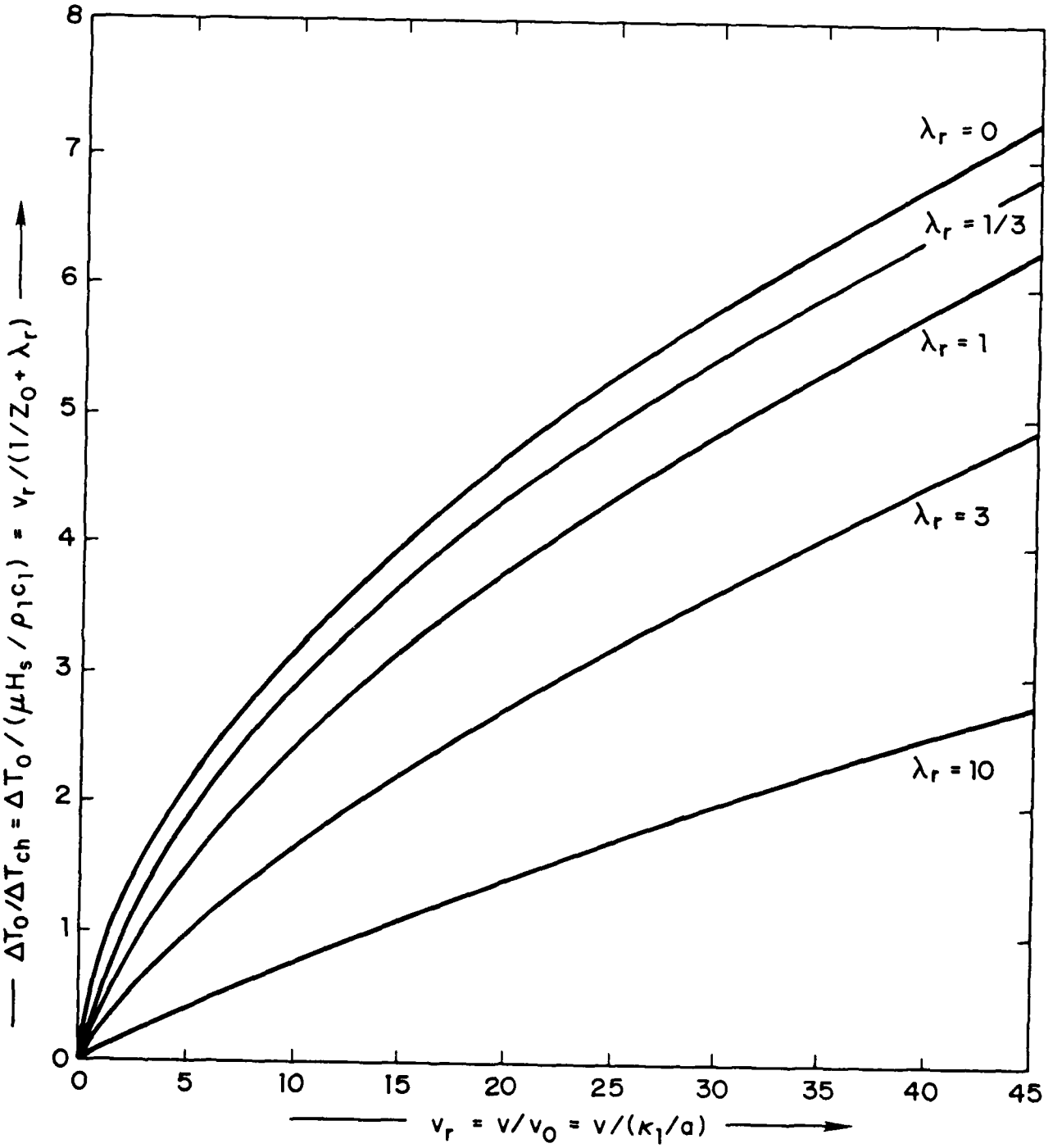
8
7
6
5
4
3
2
1
0
0
5
10
15
20
25
30
35
40
45
$\lambda_r = 0$
$\lambda_r = 1/3$
$\lambda_r = 1$
$\lambda_r = 3$
$\lambda_r = 10$
$\Delta T_0/\Delta T_{ch} = \Delta T_0/(\mu H_s/\rho_1 c_1) = v_r/(1/Z_0 + \lambda_r)$
$v_r = v/v_0 = v/(\kappa_1/a)$

Part II Fig. 3

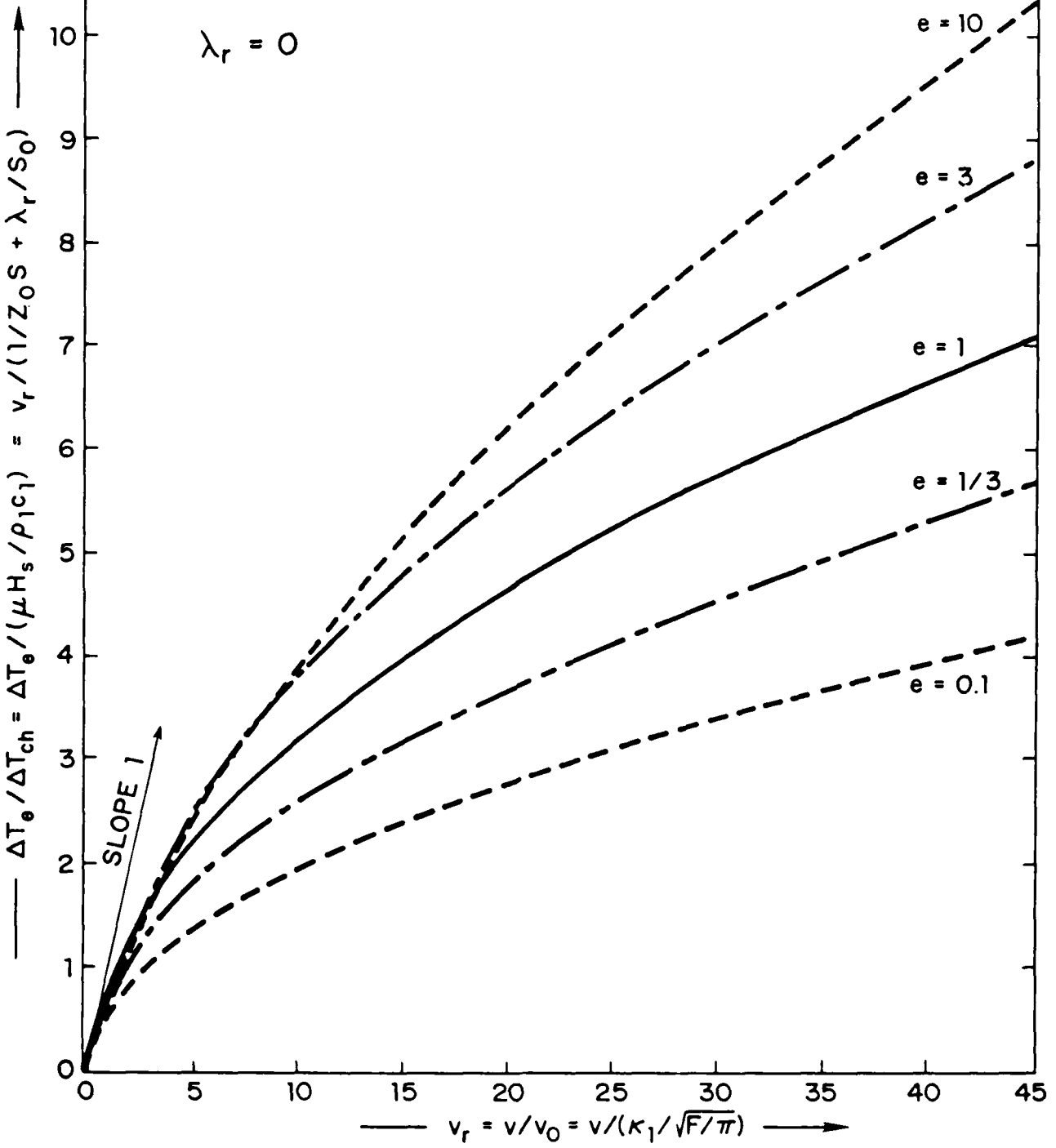
$\lambda_r = 0$
e = 10
e = 3
e = 1
e = 1/3
e = 0.1
SLOPE 1
$\Delta T_e / \Delta T_{ch} = \Delta T_e / (\mu H_s / \rho_1 c_1) = v_r / (1/Z_0 S + \lambda_r / S_0)$
$v_r = v/v_0 = v/(\kappa_1 / \sqrt{F/\pi})$
0
1
2
3
4
5
6
7
8
9
10
11
0
5
10
15
20
25
30
35
40
45

Part II Fig. 4

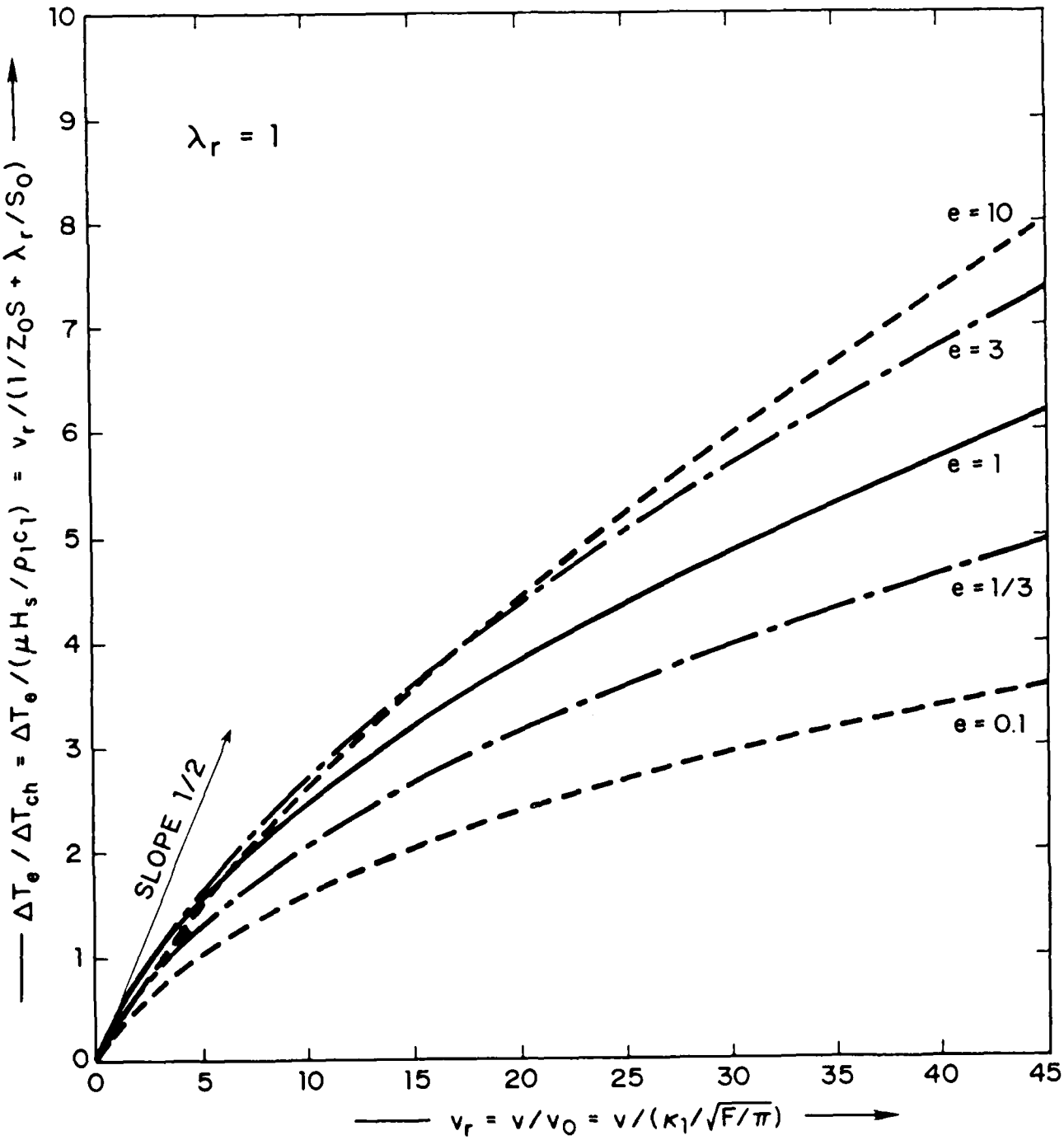
λr = 1
e = 10
e = 3
e = 1
e = 1/3
e = 0.1
SLOPE 1/2
— ΔTe / ΔTch = ΔTe / (μHs / ρ1c1) = vr / (1 / Z0S + λr / S0) —
— vr = v / v0 = v / (κ1 / √(F/π)) —
0
5
10
15
20
25
30
35
40
45
1
2
3
4
6
7
8
9

Part II Fig. 5

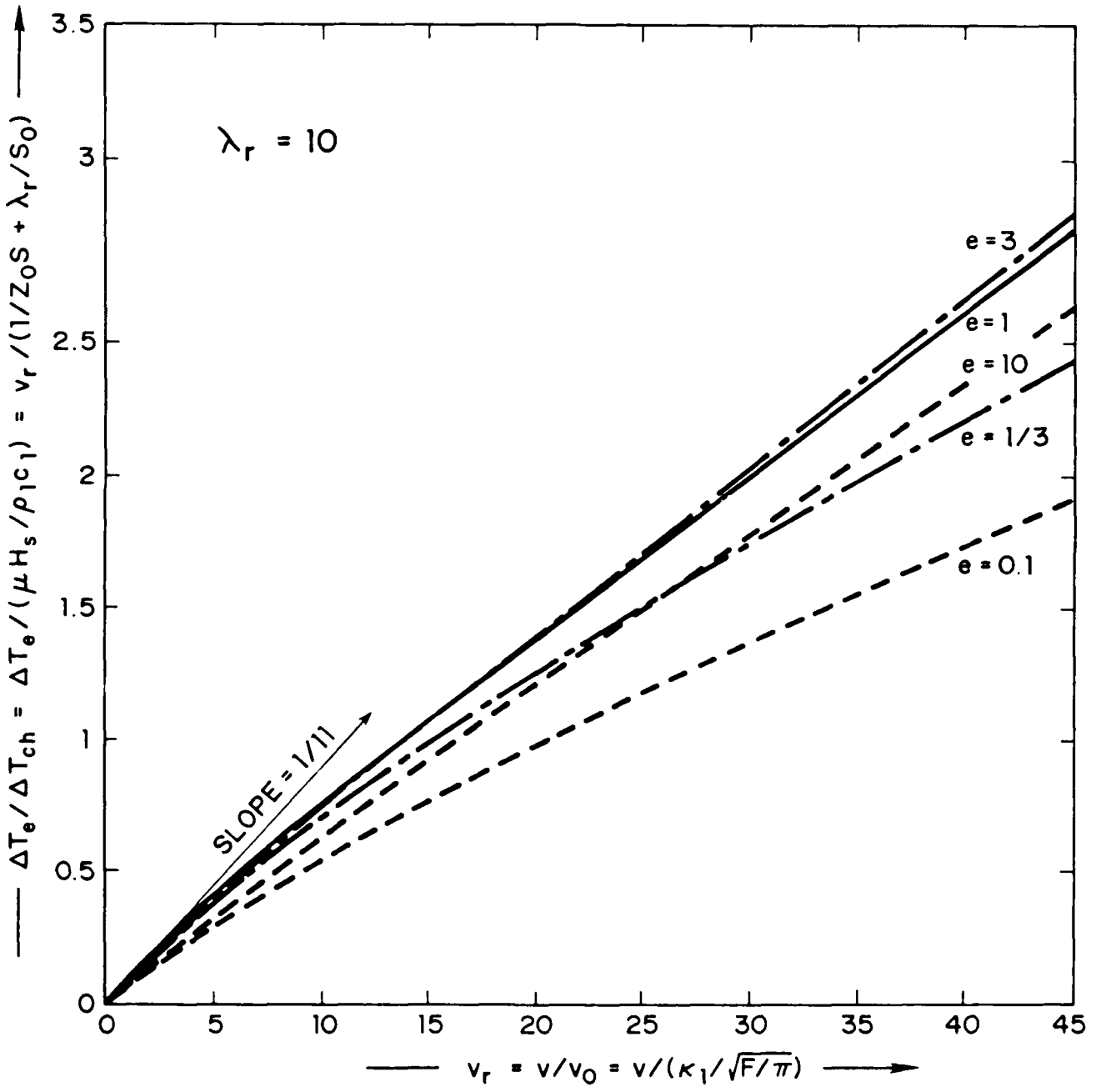
$\lambda_r = 10$
e = 3
e = 1
e = 10
e = 1/3
e = 0.1
SLOPE = 1/11
$\Delta T_e / \Delta T_{ch} = \Delta T_e / (\mu H_s / \rho_1 c_1) = v_r / (1/Z_0 S + \lambda_r / S_0)$
$v_r = v/v_0 = v/(\kappa_1 / \sqrt{F/\pi})$
0
0.5
1
1.5
2
2.5
3
3.5
0
5
10
15
20
25
30
35
40
45

Part II Fig. 6

Submitted to WEAR
(mailing date 8/29/1984)

DE-MYSTIFYING FLASH TEMPERATURES - I THEORETICAL CONSIDERATIONS

by

D. Kuhlmann-Wilsdorf
Department of Materials Science
University of Virginia
Charlottesville, VA 22901

Abstract

A simplified model, evolved in conjunction with previous theoretical work by Blok and Jaeger, yields for the flash temperature at elliptical contact spots, when the heat is uniformly developed over the contact area, $\Delta T_e = (qR/\lambda_1)/(1/Z_0 S + \lambda_r/S_0)$, where the symbols have the meaning indicated in the list of symbols. The values of the functions Z_0 and S depend on relative velocity, $v_r = v/v_0$, such that $Z_0(v_r<2) \simeq 1/(1 + v_r/3)$, and $Z_0(v_r>2) \simeq (9/8)/(\sqrt{v_r} + 1/\sqrt{8})$, and $S(v_r<1) \simeq S_0 = (4/3)/\sqrt{(1+e^{3/4}/3)(1+1/3e^{3/4})}$, and $S(v_r>1) \simeq (e^{\frac{1}{4}} + e^{\frac{1}{4}}/\sqrt{8v_r})/(1 + e^{3/4}/\sqrt{8v_r})$. These expressions are accurate to within a few percent, and they are represented graphically for some selected values by means of curves. They can be generalized for the case that the contact spot moves with velocity v_1 and v_2 relative to the two sides, respectively, as $\Delta T_e = qR/[\lambda_1/Z_0(v_{r1})S(v_{r1}) + \lambda_2/Z_0(v_{r2})S(v_{r2})$, where $v_{r1} = v_1/(\kappa_1/R)$ and $v_{r2} = v_2/(\kappa_2/R)$.

Symbols

a	radius of circular contact spot
A	length of contact spot in direction of motion
B	breadth of contact spot at right angles to direction of motion
c	specific heat
C	adjustable factor in the order of unity
$e = A/B$	axis ratio of elliptical contact spot
F	area of contact spot
K	adjustable factor in the order of unity
M	adjustable factor in the order of unity
q	heat input per unit area and time
$\dot{Q}$	rate of heat input
$R=\sqrt{F/\pi}$	characteristic dimension of contact spot
S	shape factor
S_o	shape factor at zero velocity (and up to $v_r \approx 1$)
t	time
T	temperature
ΔT	average temperature of contact spot above ambient
v	velocity
v_o	characteristic velocity ($v_o = \varkappa_1/\sqrt{F/\pi}$)
V	heated volume
Z	parameter (function of contact spot shape and velocity) needed for computing flash temperatures.
Z_o	Z for circular contact spots
$\varkappa=\lambda/\rho c$	thermal diffusivity
λ	heat conductivity
ρ	mechanical density

underlies eq. 24, is significant for $v_r = 1$. The reason for this breakdown is that forward diffusion (and correspondingly, of course, back diffusion) was neglected. Therefore the cooling of the spots is increasingly underestimated as speeds decrease. Indeed, also comparison with Jaeger's data points in Fig. 5 suggests that $v_r = 1$ is already mildly below the applicability of the theory, since these points lie noticeably below the curve for $e < 1$ and above it for $e > 1$.

Therefore, somewhat arbitrarily, for the present purposes the best values of S as computed from eq. 24 were judged to be those for $v_r = 9/8$, i.e.

$$S_{9/8} = e^{1/4}\ (1+1/3)/(1+e^{3/4}/3) = e^{1/4}(4/3)/(1+e^{3/4}/3) \qquad (29)$$

Correspondingly, S_0 was found by symmetrizing $S_{9/8}$ as

$$S_0 = \sqrt{S_{9/8}(e) \times S_{9/8}(1/e)} = (4/3)/\sqrt{(1+e^{3/4}/3)(1+1/3e^{3/4})} \qquad (30a)$$

The function S_0 has been entered in Fig. 5.

Expansion to the Case that the Contact Spot Moves Relative to Both Sides

The above flash temperatures are established almost immediately at the onset of motion. Specifically, after the spot has moved once through its whole length the equilibrium flash temperature is essentially established (10), as would indeed be expected on the basis of the theoretical derivations presented in this paper. However, it is possible, and even probable in gears, that the spot moves relative to both sides, i.e. at velocity v_1 in regard to material 1 and v_2 in regard to material 2.

In that case we may generalize eq. 1 for circular contact spots to

$$T_0 = qR/[\lambda_1/Z_0(v_{r1}) + \lambda_2/Z_0(v_{r2})] \qquad (31a)$$

with $v_{r1} = v_1/(\kappa_1/R)$ and $v_{r2} = v_2/(\kappa_2/R)$. (31b)

Clearly, $Z_{\ell o}$ as given in eq. 28 is an excellent representation of Z_o for $v_r \leq 2$ as will be seen from Fig. 4.

b) Elliptical Spots

The remaining task is to treat elliptical spots at rest or very low speeds, and to this end we must first obtain a shape factor for the stationary case and low speeds. This is necessary not only for cases in which $v_r \leq 2$, but because in regard to the asperity side the spot is stationary at all times, and we must know in which manner the heat flow $\dot{Q}_2$ is affected by shape changes.

We arrive at an approximation for the sought value $S(v=o) = S_o$ by considering Fig. 5 as follows: The values of S are clearly unsymmetrical about e = 1, so as to be higher for e than 1/e if e$>$1. This is so because spots elongated in sliding direction leave a narrower track than those elongated at right angles to the direction of motion, and thus are not as effectively cooled by the substrate. However, both lateral and forward heat diffusion increase with the length of the spot perimeter and therefore, at low speeds, elliptical contact spots are cooler than circular ones of same area, independent of axis orientation. Correspondingly, for $e \to 0$ as well as $e \to \infty$ we find S tending to zero at all speeds.

The approximation of S according to eq. 24, i.e. on the basis of the high-speed approximation, evidently is still quite good for $v_r = 1$, when the maximum value of S (and thus maximum temperature) is still found at e $>$ 1, as physically it must at all speeds $v_r > 0$. However, for values of v_r below 1/2,eq. 24 yields maxima of S for e values smaller than 1, which is certainly wrong. This indication of a noticeable error already at v_r=1 is not surprising since we know from Fig. 4 that the inaccuracy of the high-speed approximation, which

implicit assumption that rounded and rectangular spots can be treated as almost the same is vindicated by success, since S does not deviate much from unity for most reasonable values of e.

Refinement of the Theory for $v_r \lesssim 2$

a) Circular Spots

The heat diffusion pattern about a circular spot at large distances compared to a is essentially spherical at all speeds on the asperity side, and is so on the substrate side provided that $v \ll v_o$. Even so, the interfacial temperature will decrease with speed no matter how small. On the basis of the expected distortion of the diffusion pattern we may now estimate the effect of small speeds on the flash temperature as follows: On the substrate side, the effect of slow movements of the contact spot is to elongate the pattern in the direction of motion linearly with the velocity, thereby to spread out the generated heat over a larger volume, and thus to increase the heat flow into the substrate from its value of $\dot{Q}_1 = \pi\lambda_1 a\Delta T$ (see eq. 2b). The thought lies close at hand to represent this increase in $\dot{Q}_1$ by the factor $(1+Mv_r)$, where M is an adjustable factor which cannot be far from unity. We thus obtain, instead of eqs. 2 to 4,

$$\dot{Q}_1 = \pi\lambda_1 a\Delta T\ (1+Mv_r) \tag{26}$$

and, with $\dot{Q} = \dot{Q}_1 + \dot{Q}_2 = \pi a^2 q$,

$$\pi a^2 q = [\pi\ \lambda_1 a(1 + Mv_r) + \pi\lambda_2 a]\ \Delta T_o. \tag{27}$$

Comparison with Fig. 1 yields M = 1/3 and thus

$$Z_o = 1/(1 + Mv_r) = 1/(1 + v_r/3) \tag{28}$$

fitting the adjustable constant C by comparing Z_{he} with Z_{ho} for the circle (i.e. e = 1) at high speed. Namely, comparison between (21) and (22) and use of eq. 8 renders

$$Z_{he} = (9/8)e^{\frac{1}{4}}/[(1+e^{3/4}/C\sqrt{2v_r}\ )\ \sqrt{v_r}\ ] = (9/8)e^{\frac{1}{4}}/(\sqrt{v_r}+e^{3/4}/C\sqrt{2} \qquad (23a)$$

or for e = 1 and C = 2

$$Z_{ho} = (9/8)/(\sqrt{v_r} + 1/\sqrt{8}\ ) \ . \qquad (23b)$$

Fig. 4 indicates the result for Z_{ho}, i.e. for the circular spot according to eq. 23b for our initial tentative choice of C = 2. This indeed yields a remarkably good fit. Thus encouraged we introduce the shape factor

$$S = Z_{he}/Z_{ho} = e^{\frac{1}{4}}(1+1/\sqrt{8v_r})/(1+e^{3/4}/\sqrt{8v_r}) \qquad (24)$$

so that we may write, for ellipsoidal rather than circular spots, for $v_r >> (\lambda_2/\lambda_1)^2$,

$$\Delta T_{he} = S\Delta T_o \ . \qquad (25)$$

Fig. 5 shows the shape factor for a range of v_r values, including $v_r = 1$, together with the five values contained in Jaeger's work (10). These are remarkably close to those computed from eq. 24 for $v_r = 1$. This is presumably the choice made by Jaeger since he did not specify the value of v_r. At any rate there either was an oversight or an error since the shape factor certainly depends on speed. Also, Jaeger's computations of S (as indeed also for Z) were made for rectangular rather than round spots, and in this much our derived values cannot be entirely accurate. However, as seen from Fig. 5, our

above estimate of the average temperature in the quarter-ellipsoid.

Before embarking on a consideration of the effect of sideways diffusion, reflected in the $\delta B/B$ term, we examine the case of very high speeds in which it is negligible. From eq. (17) this is found as

$$\Delta T_{he} = 3Kqa/(4\rho_1 c_1 \delta z\, v) = (3K/4)q\sqrt{A}/(\sqrt{\lambda_1\rho_1 c_1}\,\sqrt{v}) \qquad (18)$$

$$= (3K/\sqrt{8})q\,\sqrt{R}\,e^{\frac{1}{4}}/(\sqrt{\lambda\,\rho_1 c_1}\,\sqrt{v}\,) \ .$$

$$\Delta T_{he} = (3K/\sqrt{8})q\sqrt{R}\,e^{\frac{1}{4}}/\sqrt{\lambda_1\rho_1 c_1}\ \sqrt{v} \ .$$

Through comparison of eq. (18) with eq. (5a) we deduce that

$K = (\sqrt{8}/3)(9/8) = 3/\sqrt{8} = 1.06$, and that in the high-speed approximation the flash temperature depends on ellipticity, e, as

$$\Delta T_{he}/\Delta T_{ho} = e^{\ 1/4} \ . \qquad (19)$$

Returning, then, to eq. (17) we rewrite it as

$$\Delta T_e/\Delta T_{he} = e^{1/4}/(1+\delta B/B) \ . \qquad (20)$$

Now with eq. 14b, eq. 20 transforms into

$$\Delta T_{he}/\Delta T_{ho} = e^{\frac{1}{4}}/(1+e^{3/4}/C\,\sqrt{2v_r}) \ . \qquad (21)$$

It is convenient to regard the above dependence of the flash temperature on the parameter C as due to a shape dependence of the function Z, writing

$$\Delta T_{he} = qRZ_{he}/\lambda_1 \qquad (22)$$

in parallelity with the first part of eq. 5a. This affords an opportunity of

$$\delta B = \delta z/C \tag{14a}$$

or

$$\delta B/B = e^{3/4}/(C\sqrt{2v_r}), \tag{14b}$$

expecting C to be in the order of 2. (We shall soon see that C = 2 is an excellent guess, when we compare the present approximation with Jaeger's results (ref. 10)).

In the present approximation we neglect forward diffusion, although it does occur and a diffusion front precedes the spot at a distance of

$$\delta A = A/8\sqrt{e}\ v_r. \tag{15}$$

The reason for this procedure is that the forward diffused heat which we neglect at the front end of the ellipsoid, is balanced by the heat that had already been deposited ahead of the midline, into the quarter-ellipsoid, by the spot in its initial position. However, this approximation, as well as that for δB according to eq. 14, and indeed the entire model, becomes invalid at speeds below v_o, or so.

The volume of the heated quarter-ellipsoid under consideration (Fig. 3) is

$$V_e = (\pi/6)AB(1+\delta B/B)\delta z = (2/3)F(1+\delta B/B)\ \delta z \tag{16}$$

whence, by the use of eq. 12

$$\Delta T_e = \tfrac{1}{2}KQ_{in}/\rho_1 c_1 V_e = 3KqA/[2\rho_1 c_1(1+\delta B/B)\delta z\ v] \quad , \tag{17}$$

where K is an adjustable factor near unity. The factor K is necessary since one can hardly expect the interfacial temperature to be exactly equal to the

presented by him, was abandoned after many hours and after the University Computer Center, having had the project under advisement for several days, declined the task. Therefore, we shall give a simple estimate, applicable to $v_r \geq 2$ or perhaps even $v_r \geq 1$, by refining the model already used to derive eq. 5:

By geometry, about one half of the heat

$$Q_{in} = AFq/v, \tag{12}$$

developed while the contact slides once through its whole length A, is distributed in a volume whose shape is included in a diffusion front as sketched in Fig. 3. The average temperature in the outlined quarter-ellipsoid is representative of the contact spot temperature, within some factor not far from unity, according to the previous derivation of ΔT_{ho} (eq. 5). The sideways extension of the ellipsoid beyond the width of the track swept out, δB, is due to lateral diffusion, and its short axis, δz, is due to inward diffusion. Much as before, seeing that inward diffusion occurs during time interval A/v, we estimate δz as

$$\delta z = \sqrt{\kappa_1 A/v} = A/(e^{\frac{1}{4}}\sqrt{2v_r}) \quad . \tag{13}$$

Clearly, δB is some fraction of δz since, firstly, lateral diffusion of significance begins only after the contact spot has reached the mid-way position and, secondly, the heat content outside the geometrical limits of the swept track of width B is fed only very ineffectively after the perimeter of the spot shrinks away from them once again. On the other hand, δB consists of <u>two</u> strips, one at either side of the track.

Thus we write

Further we redefine the characteristic velocity v_o as

$$v_o = \kappa_1/\sqrt{F/\pi} = \kappa_1/R \qquad (10)$$

in general, which we met already for circular spots, in particular, as $v_o = \kappa_1/a$.

It is mostly helpful and instructive to use relative velocities $v_r = v/v_o$, rather than absolute values. The significance of v_o is that, in the substrate, at velocity v_o, the contact spot and diffusion front emitted at time t=0 both traverse the characteristic distance, R, in the characteristic time interval

$$\delta t = R/v_o = R^2/\kappa_1, \qquad (11a)$$

i.e.

$$v_o \delta t = \sqrt{\kappa_1 \delta t} = R. \qquad (11b)$$

Essentially, therefore, at speeds much below v_o heat diffusion in the substrate keeps up with the contact spot. Conversely, at $v \gg v_o$, as far as the contact spot is concerned, the heat is left behind in the substrate where it was first deposited. It is thus v_o in regard to which v has to be either small or large to generate the low and high speed cases already discussed.

The Effect of Contact Spot Shape at $v_r \geq 2$ When the Asperity Side is an Insulator

No straight-forward, simple treatment of the effect of contact spot shape on flash temperature is available. Jaeger (10), Holm (4) and Shobert (5) have considered it mathematically to some extent, but their equations are cumbersome, to say the least, and it is difficult to find specific answers to actual cases from these. Indeed, an initial attempt at computing a number of representative values from the equations given by Jaeger (10), beyond the few

$$Q_{in} = (\pi a^2 q) 2a/v \qquad (6)$$

is deposited. Underneath the spot, the heat meanwhile had time to diffuse only through a thickness in the order of $\sqrt{\kappa_1 2a/v} \ll a$, and thus it is essentially dispersed in a volume

$$V \simeq 4a^2 \sqrt{\kappa_1 2a/v} \quad . \qquad (7)$$

The interfacial temperature rise must be comparable to the average temperature rise calculated for that volume since, on the one hand, not all of the heat energy is confined to the volume V and, on the other hand, the interface is hotter than the average temperature in V. Therefore

$$\Delta T_{ho} \simeq Q_{in} / (\rho_1 c_1 V) = (\pi/\sqrt{8})\, q\sqrt{a}/(\sqrt{\lambda_1 \rho_1 c_1}\ \sqrt{v}\ ) \qquad (5b)$$

which is to be compared with eq. 5a. We thus found in the high-speed limit for circular contacts $Z_{ho} \simeq 1.1 \sqrt{\kappa_1/av}$ which is fortuitously close to the actual answer embodied in Fig. 2, namely

$$Z_{ho} = (9/8) \sqrt{\kappa_1/av} = (9/8)/\sqrt{v/v_o} = (9/8)/\sqrt{v_r} \quad . \qquad (8)$$

Characteristic Dimension, Velocity, and Distance Between Spot and Thermal Diffusion Front

In general a contact spot will not be circular but roughly elliptical, with axes lengths A and B, say, in the direction parallel and at right angles to the direction of motion. The ellipticity of the spot shall be called $e = A/B$ and its area F, so that we may define the characteristic dimension of the spot as

$$\sqrt{F/\pi} = \tfrac{1}{2}\sqrt{AB} = \tfrac{1}{2}A/\sqrt{e} = R \quad . \qquad (9)$$

we find

$$\Delta T_o = qa/(\lambda_1 + \lambda_2) \qquad (4)$$

for the contact spot at rest. Comparing eqs. 1 and 4 shows thus that at rest, or at small speeds, $Z_o = 1$, in agreement with Fig 2.

c) The Limiting Case of Very High Speeds

When the asperity slides over the substrate, it continuously encounters cool substrate and leaves a trail of warmed material behind, much like the contrail of an airplane. At very low speeds the extra heat energy needed to heat up that trail is negligibly small compared to the radial heat diffusion of the stationary case just discussed. But as the heated volume increases, so does the heat left behind in the trail. Thus with rising velocity the contact spot is increasingly cooled by the substrate, until the heat absorbed in the trail becomes dominant at high speeds. At given q, therefore, ΔT decreases with speed, mediated through the corresponding decrease of Z and, depending on λ_1/λ_2, sooner or later the heat flow into the asperity side becomes negligible.

For that case, i.e. $\dot{Q}_2 \ll \dot{Q}_1$, from eq. 1 in conjunction with Fig. 2 and introducing the relative speed $v_r = v/v_o = v/(\kappa_1/a)$, one finds directly

$$\Delta T\ (v_r \gg 1) = \Delta T_{ho} = qaZ_{ho}/\lambda_1 = (9/8)\ qa/\lambda_1\sqrt{v_r} = (9/8)\ q\sqrt{a}/(\sqrt{\lambda_1\rho_1 c_1}\ \sqrt{v}). \qquad (5a)$$

We may readily derive this result semi-quantitatively as follows: Consider the heat flow into the substrate while the contact spot moves at high speed through the distance 2a, in time 2a/v, generating $(2a)^2$ of new trail area, while the heat

where the subscripts 1 and 2 designate a substrate (1) and flat asperity (2), respectively, as sketched in Fig. 1. Here λ stands for heat conductivity, q is the amount of heat developed per unit area of contact spot per unit time, and Z_o is a numerically known function of velocity. The subscript o is carried as a reminder that the function Z_o and the above temperature rise T_o apply to circular contact spots only.

Eq. 1 was derived from the early work of Block (8,9) as elaborated by Jaeger (10,11). The function Z_o is indicated in Fig 2 as extracted from Fig. 7 of ref. 10.

b) The Limiting Case of Very Low Speeds

The asperity side is stationary in regard to the contact spot at all times. If it is circular of radius a, heat diffuses into the material of the asperity side at the rate

$$\dot{Q}_2 = \pi \lambda_2 a \Delta T, \tag{2a}$$

if the interface is at temperature ΔT above ambient, regardless of relative velocity. To the extent that the bulk temperatures of the two sides are equal, as is assumed throughout, and that ideal thermal contact exists between them at the contact spot, then at rest, i.e. for velocity v = 0, the heat flow into the substrate must be similarly

$$\dot{Q}_1 = \pi \lambda_1 a \Delta T. \tag{2b}$$

Since the total heat flow is the sum of those two parts, i.e.

$$\dot{Q}_1 + \dot{Q}_2 = \dot{Q} = \pi a \Delta T (\lambda_1 + \lambda_2) = q \pi a^2, \tag{3}$$

to a lack of simple methods to compute, or at least estimate, them. In regard to the latter, one is painfully aware that the scientist will ordinarily disdain numerical estimates and regard quantitative data the more highly, the more accurately they are known. In regard to flash temperatures that would be an unjustifiable attitude, though. In actual fact, numbers and average sizes of contact spots change from moment to moment, and any individual contact spot, as long or briefly as it may last, does not only change its size and shape, and hence its temperature, within short time intervals, but also experiences erratic changes in the momentary temperature distribution over its area. Therefore, while it is possible to calculate the temperature distribution over any specific contact spot once its size, speed, shape and the nature and thickness of intervening surface layers or lubrication layers are known, what would be the benefit thereof unless one felt confident that one dealt with *the representative contact spot*? *It is the average contact spot*, therefore, after which one should enquire, and one must realize that actual flash temperatures will widely fluctuate about the value calculated for it.

In this spirit, then, we shall develop some simple equations to aid in such calculations. In Parts II and III we shall then consider practical applications and give some sample values, expanding on previous work (6-7)

Basic Equations

a) The General Equation for Circular Contact Spots

For circular contact spots of radius a, one may write for the average flash temperature (6,7)

$$\Delta T_o = qa/(\lambda_1/Z_o + \lambda_2) \qquad (1)$$

DE-MYSTIFYING FLASH TEMPERATURES - I THEORETICAL CONSIDERATIONS

by

D. Kuhlmann-Wilsdorf
Department of Materials Science
University of Virginia
Charlottesville, VA 22901

Introduction

The temperature rise at contact spots during sliding between two solids with or without simultaneous current flow has great significance in a number of ways, and some well-known papers addressed to the non-mathematician are available (e.g. refs. 1-3). Thus temperature spikes at contact spots induce thermal stresses which on repeated contacts can cause fatiguing; they mostly cause superficial softening and thus reduction of the friction; they can cause the formation or dissolution of precipitates; can anneal out surface modifications such as through ion implantation; will generally enhance surface reactions, especially oxidation; will enhance diffusion into and out of surfaces so as to cause surface decarburization of steels, for example; and under suitable circumstances can cause phase transformations. An important factor in the enumerated temperature effects, especially in regard to chemical reactions, diffusion, and changes in precipitates, is the fact that cooling is typically so rapid that the thermal equilibrium vacancy concentration of the flash temperature is essentially frozen in. Correspondingly these phenomena can be enhanced much beyond the expectations on the basis of the time-temperature history at the contact spots alone.

In spite of the above, and in spite of the already cited papers plus the important work by Holm (4) and Shobert (5), much uncertainty and confusion exists regarding the magnitude of flash temperatures. Presumably this is due

δB increase of track width at trailing end of contact spot due to lateral diffusion of heat

δz thickness of heated layer underneath contact spot

Subscripts

e pertaining to elliptic contact spots

h pertaining to high speeds ($v_r \gg 1$)

ℓ pertaining to low speeds and to rest ($v_r \ll 1$)

o pertaining to circular contact spots (except in the case of v_o which applies also to elliptical spots)

1 pertaining to the substrate

2 pertaining to the asperity side

Further, on the basis of the considerations in the preceding section we obtain for elliptical contact spots in that case

$$\Delta T_e = qR/[\lambda_1/Z_o(v_{r1})S(v_{r1}) + \lambda_2/Z_o(v_{r2})S(v_{r2})]. \quad (32)$$

Summarizing Conclusions

The accuracy with which the present simple theory reproduces Jaeger's(10) theoretical results is most reassuring and inspires confidence that the model effectively represents the physics involved. If we accept the flash temperature of the circular spot at rest with insulating asperity-side, of value $q/\sqrt{F/\pi}/\lambda_1$, as basic, it is reasonable and convenient to express all flash temperatures as fractions thereof. Namely, under no circumstances does the flash temperature rise above the mark of $qa/\lambda_1 = q/\sqrt{F/\pi}/\lambda_1$.

For circular spots in motion with a non-insulating asperity side of thermal conductivity λ_2, naming $\lambda_2/\lambda_1 = \lambda_r$, we may then write

$$\Delta T_o/(q\sqrt{F/\pi}\ /\lambda_1) = 1/(1/Z_o+\lambda_r). \quad (33)$$

As was shown, in accordance with eqs. 23 b and 28 and demonstrated in Fig. 4, Z is well represented by

$$Z_o(v_r \leq 2) = Z_{\ell o} = 1/(1 + v_r/3) \quad (28)$$

and

$$Z_o(v_r \geq 2) = Z_{ho} = 9/8/(\sqrt{v_r} + 1/\sqrt{8}\ ) . \quad (23c)$$

The maximum error with this approximation is about 3% at $v_r = 2$, as seen in Fig. 4.

Fig. 6 shows ΔT_o for a few values of λ_r between 0 (i.e. insulating asperity) and $\lambda_r = 10$ (i.e. the thermal conductivity of the substrate is only 10% of that of the asperity side). From this in conjunction with Fig. 2 it is

evident that the high-speed limit, in which the bulk of the heat is absorbed by the substrate, is already fairly well approximated at $v_r \approx 2$ for $\lambda_r = 0$, but only for much higher speeds at larger values of λ_r. In fact for the high-speed approximation to be useable, it must be $v_r \gg \lambda_r^2$.

The effect of ellipticity is expressed in terms of the shape factor S. For $v_r \leq 1$ it is approximately equal to S_o, as given in eq. 30a or, in a slightly different but not superior formulation,

$$S\ (v_r \leq 1) \approx S_o = (4/3)\sqrt{(10/9) + e^{3/4}/3 + 1/3e^{3/4}}\ . \qquad (30b)$$

Thus, at slow speeds the shape factor applying to the substrate is S_o, the same as for the asperity side. For elliptical shapes (including, of course, circles with e = 1) at low speed we therefore obtain

$$\Delta T_{\ell e}/(q\sqrt{F/\pi}\ /\lambda_1) = S_o/(1/Z_{\ell o}+\lambda_r) = S_o/(1 + v_r/3 + \lambda_r)\ . \qquad (34)$$

For higher speeds though, as certainly for $v_r > 1$, the shape factor S applies to the substrate but S_o continues to apply to the asperity side, so that

$$\Delta T_e/(q\sqrt{F/\pi}\ /\lambda_1) = 1/(1/Z_o S + \lambda_r/S_o). \qquad (35)$$

Figs. 7, 8 and 9 show the flash temperature computed according to eqs. 34 and 35, whereby between $v_r = 0.2$ and $v_r = 1$ the transition between S_o and S has been smoothed. It is interesting to note how e values above unity lift the flash temperatures above that for circular spots at higher speeds, and how those speeds at which ΔT_e is larger than ΔT_o increase with increasing e values and, for same e, with increasing λ_r. Conversely, at low speeds any ellipticity reduces the flash temperature, and does so by the same amount for e and 1/e. For $e < 1$ the factor by which the temperature is reduced increases with increasing speed. Even so, the effect of ellipticity, whether e is above or

below unity, is non-major for all speeds below $v_r \simeq 100$, staying within a factor of two, more or less, of that for circular spots, at all values of v_r below 100 for $0.1 \leq e \leq 10$.

Acknowledgements

The financial support of this research through the Materials Division (Tribology) of the Office of Naval Research, Arlington, VA is gratefully acknowledged.

References

1) J. F. Archard, Wear 2 (1958/9) 438.

2) E. Rabinowicz, Friction and Wear of Materials, Wiley, New York, 1965, pp. 87-91.

3) E. Rabinowicz, Wear, 78 (1982) 29.

4) R. Holm. Electric Contacts, Springer Verlag (4th Edition), Berlin/New York, 1967.

5) E. I. Shobert, Carbon Brushes, Chemical Publishing Co., Inc. New York, 1965.

6) D. Kuhlmann-Wilsdorf, Electrical Contacts-1983, Proc. 29th Holm Conf., Ill. Inst. Techn., Chicago, p. 21.

7) D. Kuhlmann-Wilsdorf, IEEE Transact. on Magnetics, Vol. MAG-20, No. 2 (1984) p. 340.

8) H. Blok, Proc. General Disc. on Lubrication and Lubricants, Inst. Mech.Eng., 2 (1937) 14.

9) H. Blok, Ann. N.Y. Acad. Sci., 53 (1951) 779.

10) J. C. Jaeger, J. Proc. Roy. Soc. N.S.W. 56 (1942) 203.

11) H. S. Carslaw and J. C. Jaeger, The Conduction of Heat in Solids, Oxford University Press, (2nd Edition) London 1959.

Legends

Fig.1) Mathematical model of a contact spot, consisting of a flat circular or elliptical asperity of material 2 with thermal conductivity λ_2, sliding with velocity v on a semi-infinite substrate of material 1 with thermal conductivity λ_1.

Fig.2) The parameter Z_o as a function of relative velocity $v_r = v/v_o$ for a circular contact spot as extracted from Jaeger's calculation according to Fig. 7 of ref. 10. Also indicated are the high-speed limit $Z_{ho} = (9/8)/\sqrt{v_r}$ and the low speed limit of unity given in ref. 10.

Fig.3) Model of the volume (roughly a quarter-ellipsoid) about an elliptical contact spot (with axes A and B) which receives about one half of the heat energy developed while the spot slides once through its length A.

Fig.4) The function $Z_{ho} = (9/8)/(\sqrt{v_r} + 1/\sqrt{8})$, applicable for $v_r \geq 2$, and the function $Z_{\ell o} = 1/(1+v_r/3)$ applicable for $v_r \leq 2$, in accordance with eqs. 23b and 28.

Fig.5) The shape factor $S = e^{\frac{1}{4}}(1+1/\sqrt{8v_r})/(1+e^{3/4}/\sqrt{8v_r})$, and the shape factor $S_o = 4/3/\sqrt{(1+e^{3/4}/3)(1+1/3e^{3/4})}$ for stationary spots according to eqs. 24 and 30a, respectively. S_o is applicable to $v_r \leq 1$ and S to $v_r \geq 1$. Included are values given by Jaeger (ref. 10) for rectangular contact spots (symbol ■)presumed to be applicable to $v_r = 1$.
The shape factor corrects the function Z_o for application to elliptical contact spots. Namely for $v_r \geq 1$ it is $Z_{he} \simeq SZ_{ho}$ and for $v_r \leq 1$ it is $Z_{\ell e} \simeq S_o Z_o$, where Z_{ho} and $Z_{\ell o}$ are as shown in Fig. 4.

Fig.6) The flash temperature of a circular contact spot in units of $q\sqrt{F/\pi}/\lambda_1$, i.e. as fraction of the temperature which that spot would have at rest when the asperity side is an insulator, as a function of relative velocity for different values of $\lambda_r = \lambda_2/\lambda_1$. Large values of λ_r mean that the asperity side is a much better conductor than the substrate and thus conducts away much of the heat.

Fig.7) The flash temperature for contact spots of different shapes in units of $q\sqrt{F/\pi}/\lambda_1 = qR/\lambda_1$ (i.e. as fraction of the temperature which a circular spot of same area would have at rest when the asperity side is an insulator) for $\lambda_r = \lambda_2/\lambda_1 = 0$ (meaning in this case the asperity side <u>is</u> an insulator). Ellipticities $e = A/B > 1$ mean spots elongated in sliding direction and $e < 1$ spots flattened in sliding direction.

Fig.8) As Fig. 7 but for $\lambda_r = 1$, *meaning* that the heat conductivities on the two sides are equal.

Fig.9) As Fig. 7 but for $\lambda_r = 10$, i.e. the case in which the asperity side is a ten times better conductor than the substrate.

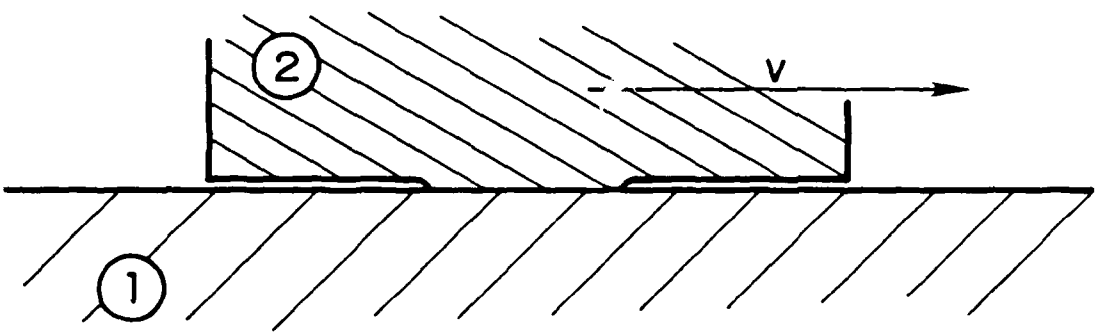

Part I Fig. 1

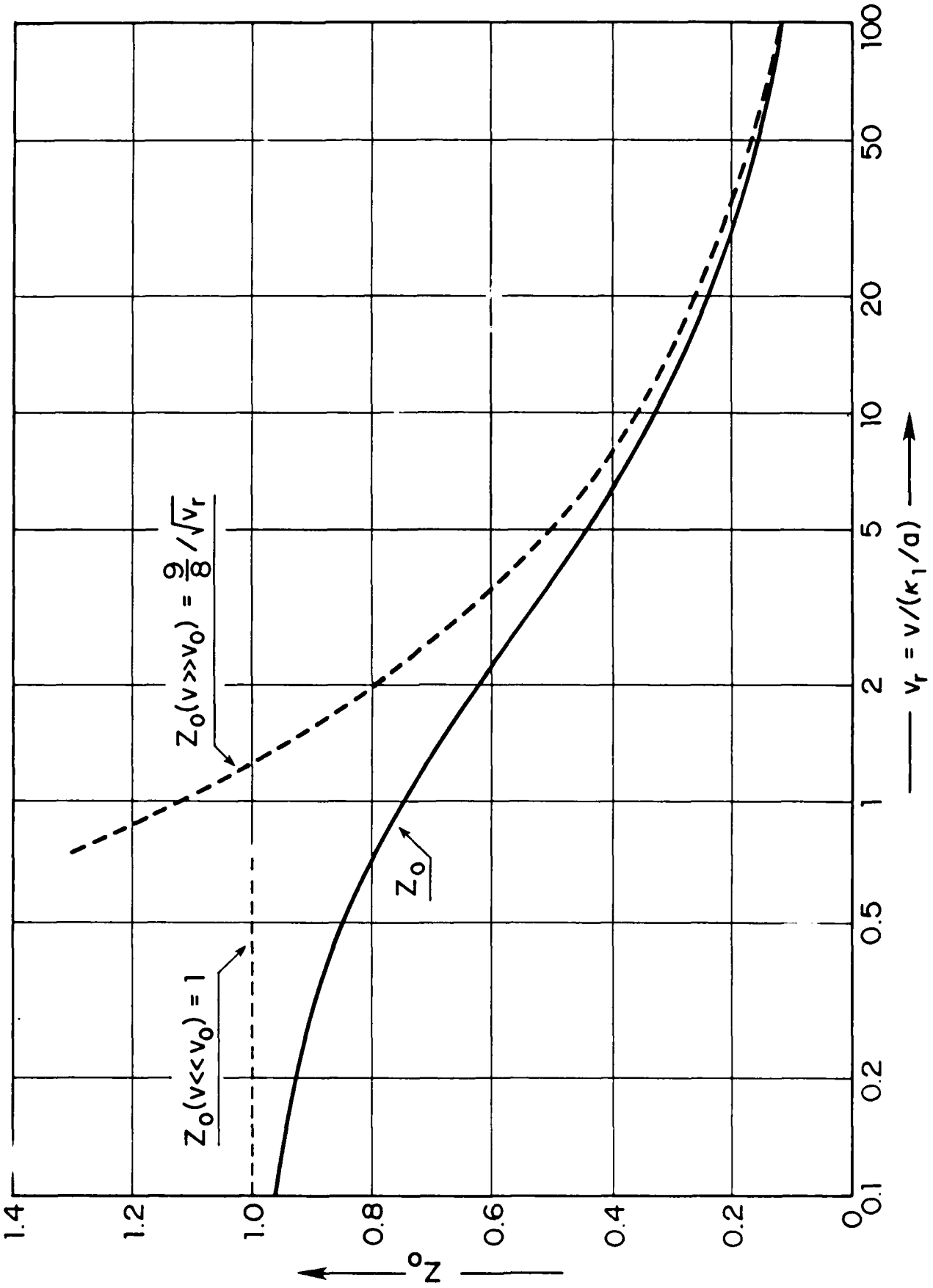
$Z_o(v>>v_o) = \frac{9}{8}/\sqrt{v_r}$
Z_o
$Z_o(v<<v_o) = 1$
Z_o
$v_r = v/(\kappa_1/a)$
1.4
1.2
1.0
0.8
0.6
0.4
0.2
0
0.1
0.2
0.5
1
2
5
10
20
50
100

Part I Fig. 2

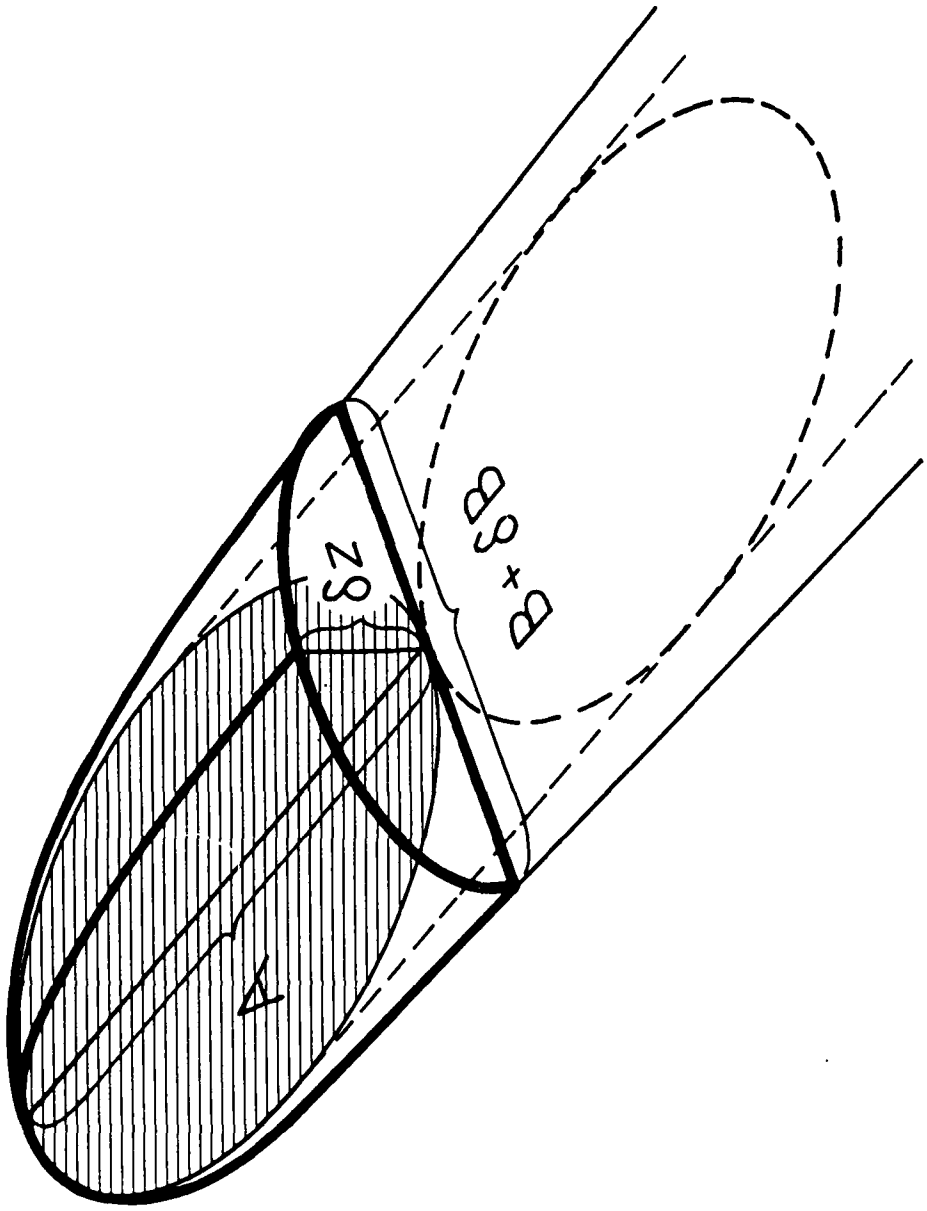

Part I Fig. 3

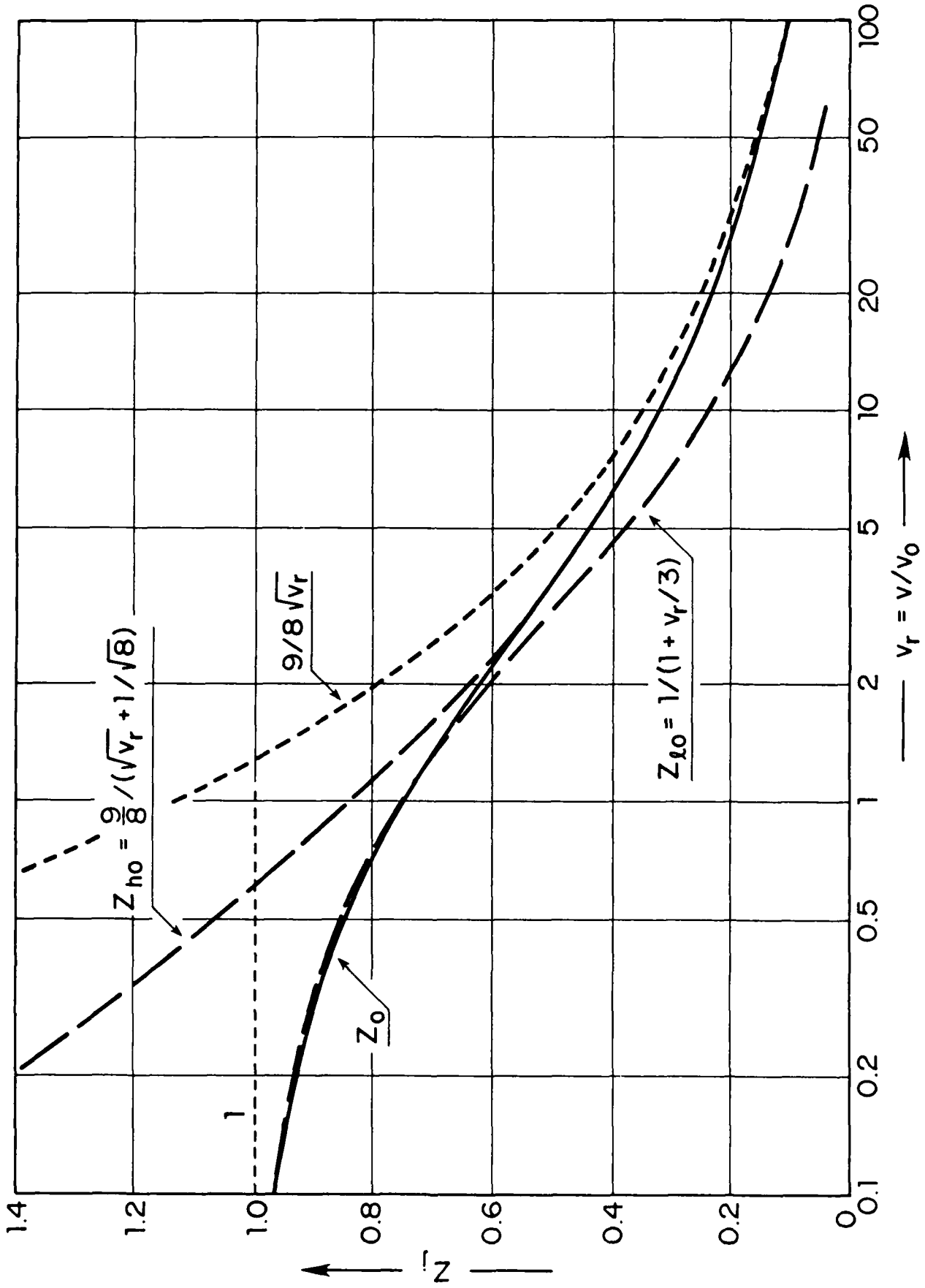
1.4
1.2
1.0
0.8
0.6
0.4
0.2
0
Z_j
1
$Z_{ho} = \frac{9}{8}/(\sqrt{v_r} + 1/\sqrt{8})$
$9/8\sqrt{v_r}$
Z_0
$Z_{10} = 1/(1 + v_r/3)$
0.1
0.2
0.5
1
2
5
10
20
50
100
$v_r = v/v_0$

Part I Fig. 4

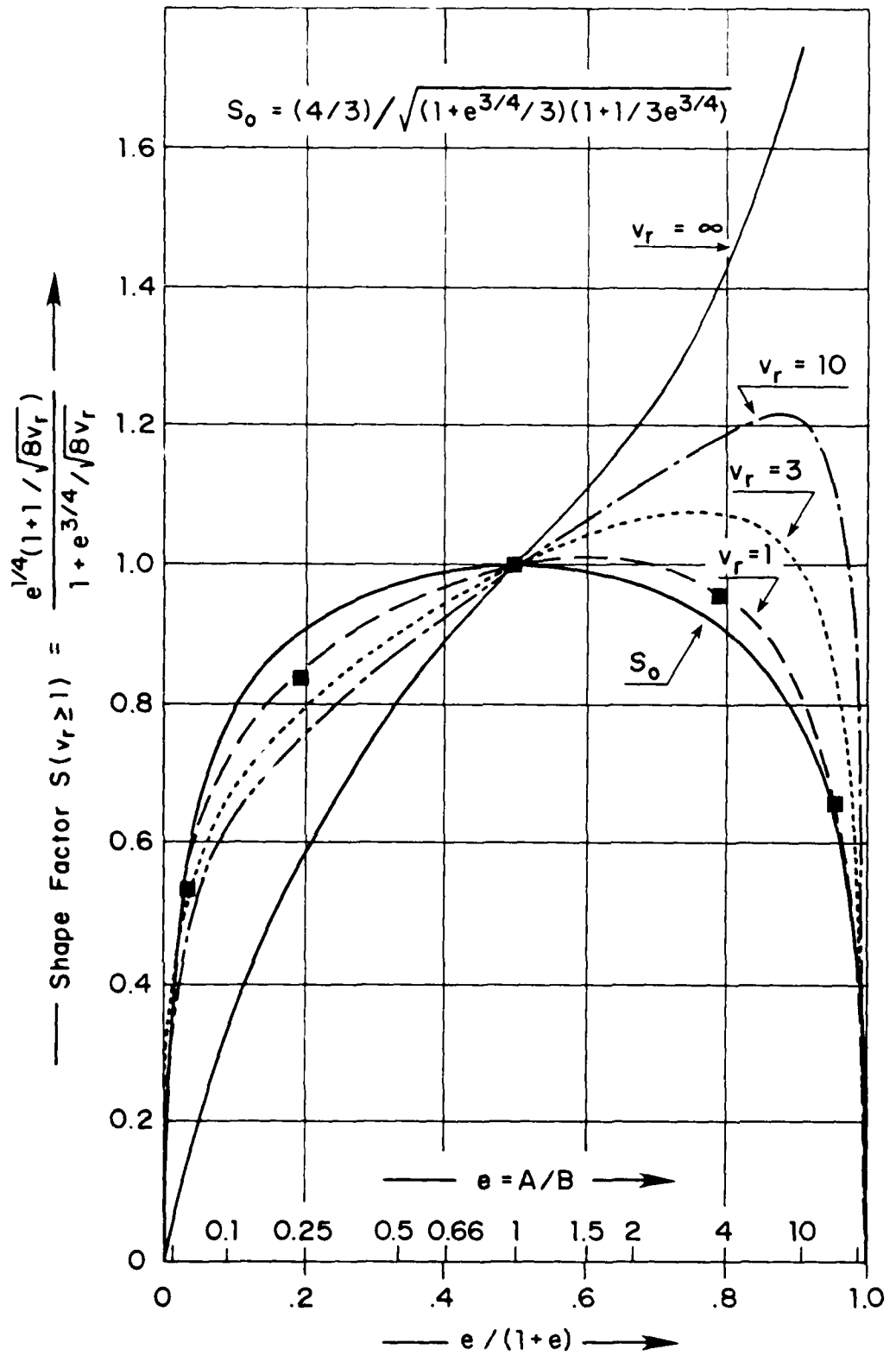
$S_o = (4/3)/\sqrt{(1+e^{3/4}/3)(1+1/3e^{3/4})}$
$v_r = \infty$
$v_r = 10$
$v_r = 3$
$v_r = 1$
S_o
Shape Factor $S(v_r \geq 1) = \frac{e^{1/4}(1+1/\sqrt{8v_r})}{1+e^{3/4}/\sqrt{8v_r}}$
1.6
1.4
1.2
1.0
0.8
0.6
0.4
0.2
0
e = A/B
0.1 0.25 0.5 0.66 1 1.5 2 4 10
0 .2 .4 .6 .8 1.0
e / (1+e)

Part I Fig. 5

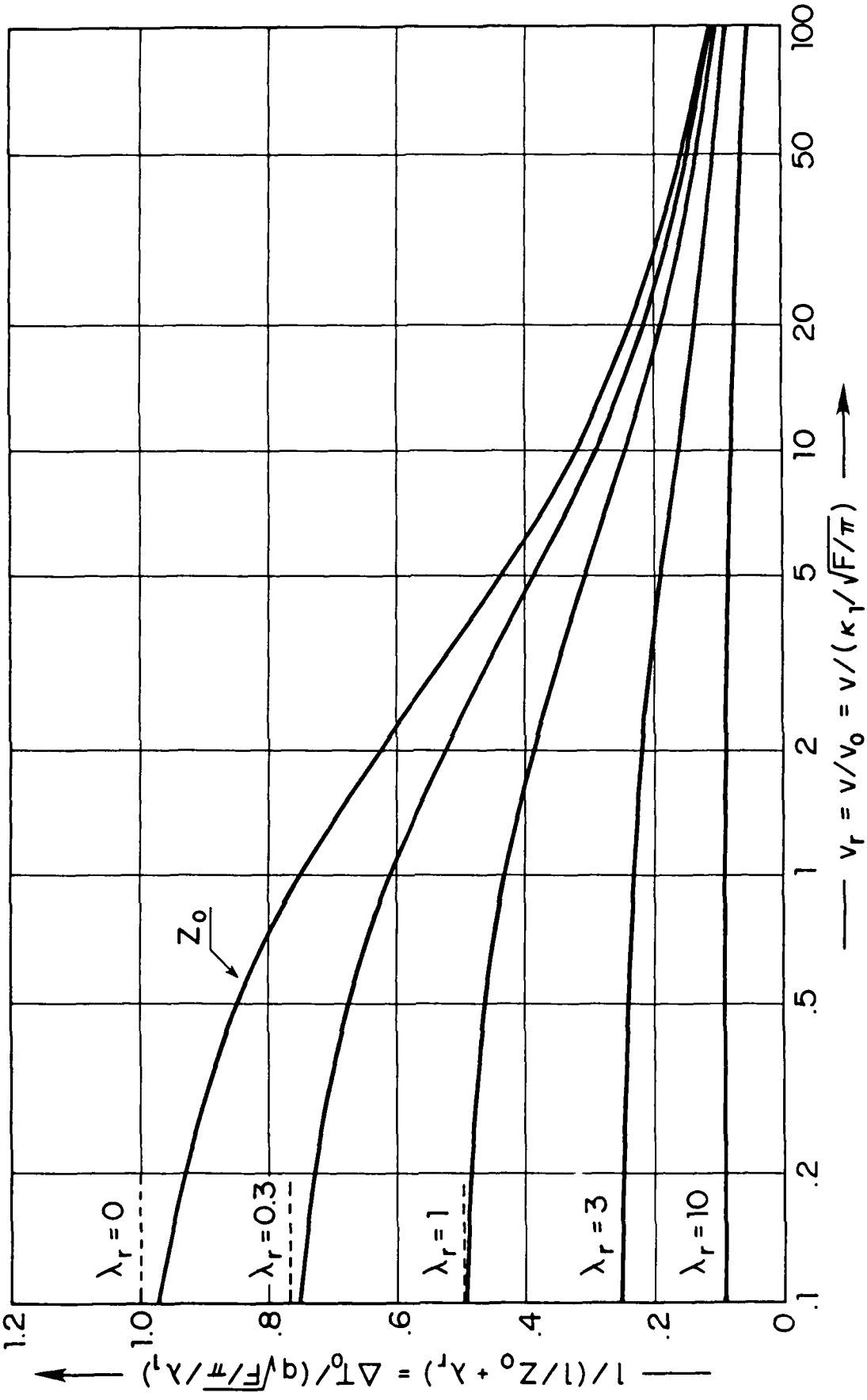
$\Delta T_0/(q\sqrt{F/\pi}/\lambda_1) = 1/(1/Z_0 + \lambda_r)$
$v_r = v/v_0 = v/(\kappa_1/\sqrt{F/\pi})$
Z_0
$\lambda_r = 0$
$\lambda_r = 0.3$
$\lambda_r = 1$
$\lambda_r = 3$
$\lambda_r = 10$
1.2
1.0
.8
.6
.4
.2
0
.1
.2
.5
1
2
5
10
20
50
100

Part I Fig. 6

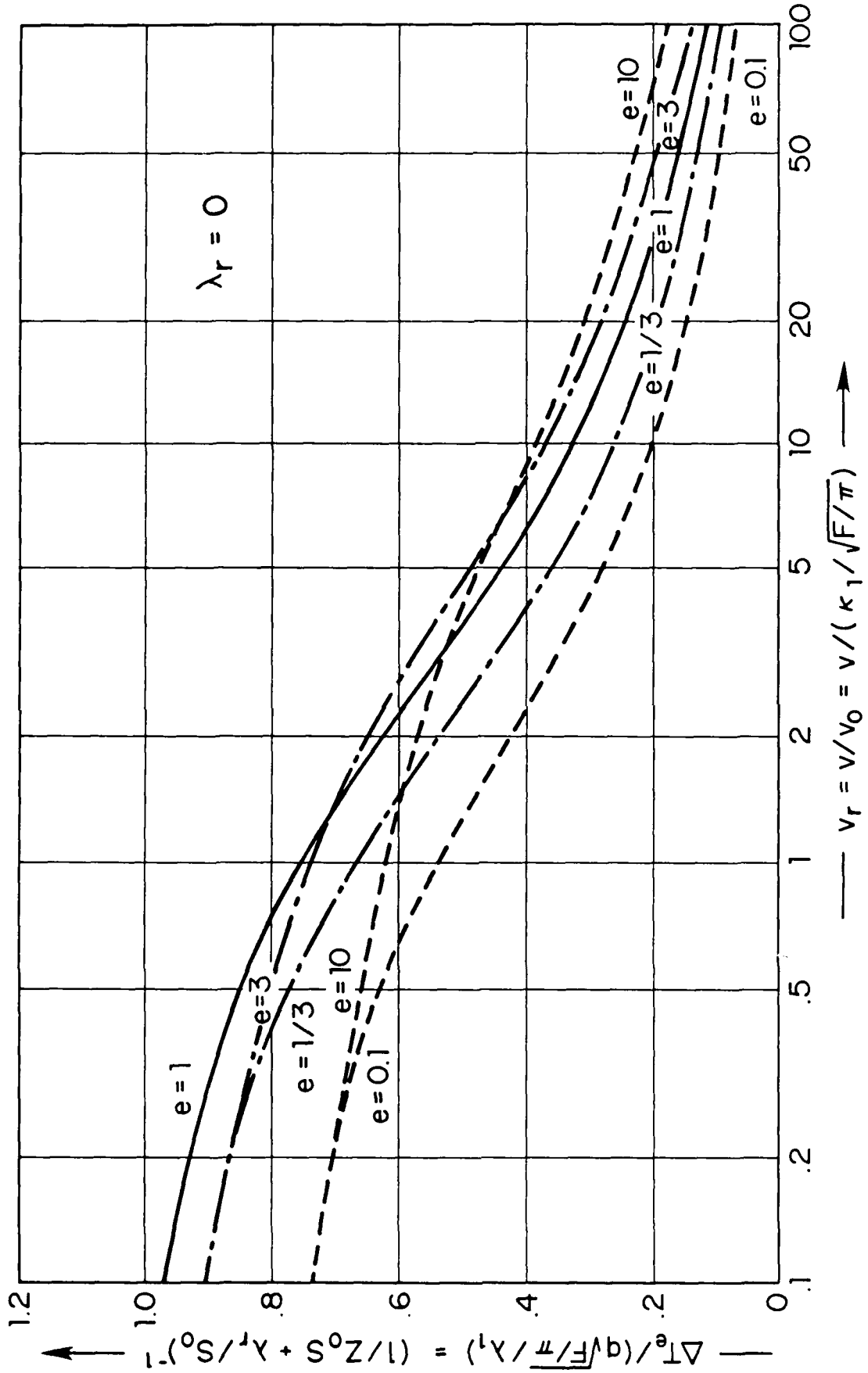
$\lambda_r = 0$
e=10
e=3
e=1
e=1/3
e=0.1
e=1
e=3
e=10
e=1/3
e=0.1
$\Delta T_e/(q\sqrt{F/\pi}/\lambda_1) = (1/Z_0S + \lambda_r/S_0)^{-1}$
$v_r = v/v_0 = v/(\kappa_1/\sqrt{F/\pi})$
0
.1
.2
.5
1
2
5
10
20
50
100
.2
.4
.6
.8
1.0
1.2

Part 1 Fig. 7

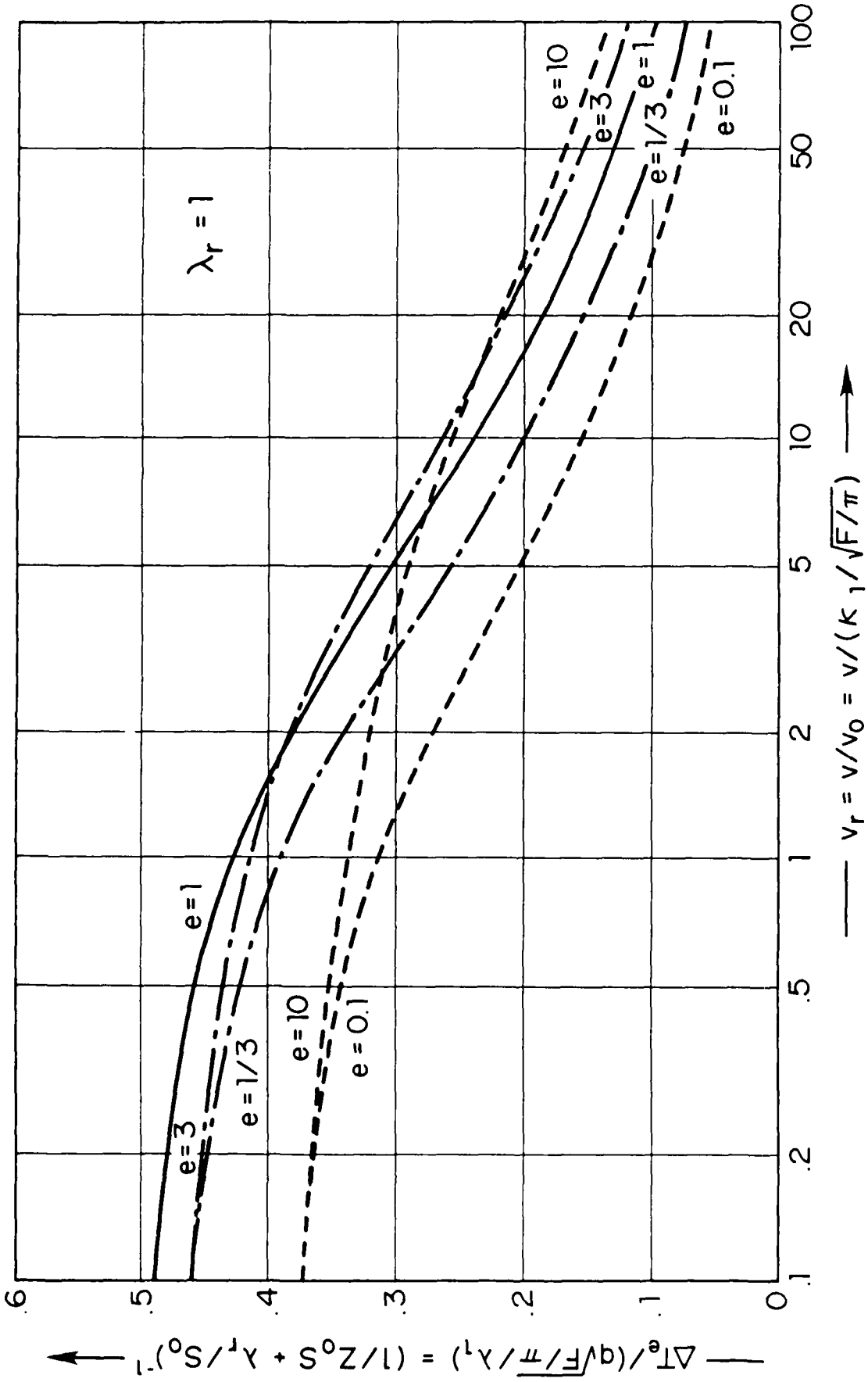
$\lambda_r = 1$
e=10
e=3
e=1
e=1/3
e=0.1
e=1
e=3
e=1/3
e=10
e=0.1
$v_r = v/v_o = v/(K_1/\sqrt{F/\pi})$
$\Delta T_e/(qv\sqrt{F/\pi}/\lambda_1) = (1/Z_oS + \lambda_r/S_o)^{-1}$
0
.1
.2
.5
1
2
5
10
20
50
100
1
2
3
4
5
6

Part I Fig. 8

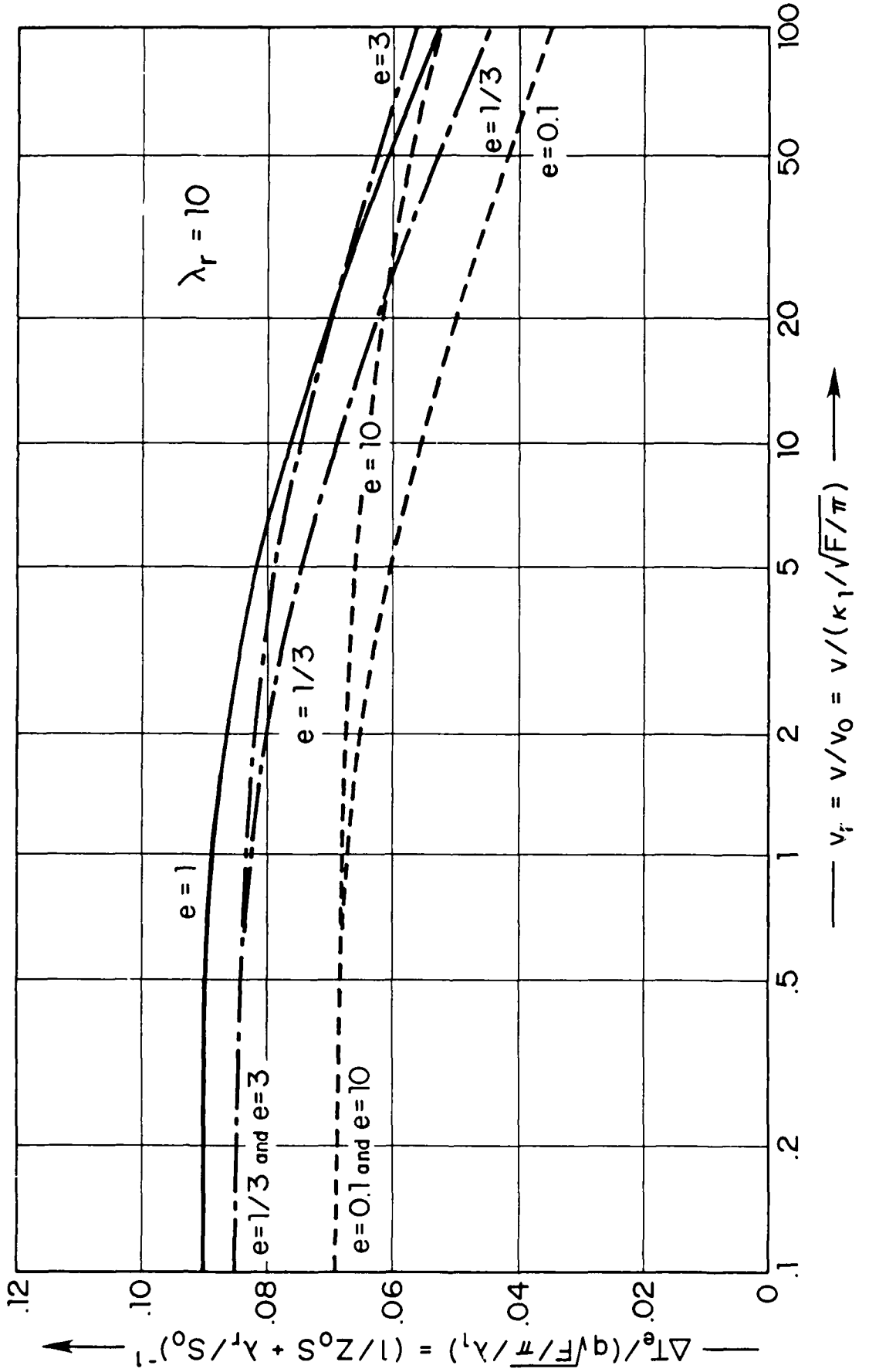
$\lambda_r = 10$
e=3
e=1/3
e=0.1
e = 10
e = 1/3
e = 1
e=1/3 and e=3
e=0.1 and e=10
$\Delta T_e/(q\sqrt{F/\pi}/\lambda_1) = (1/Z_0S + \lambda_r/S_0)^{-1}$
$v_r = v/v_0 = v/(\kappa_1/\sqrt{F/\pi})$
.12
.10
.08
.06
.04
.02
0
.1
.2
.5
1
2
5
10
20
50
100

Part I Fig. 9

WEAR OF MATERIALS - 1985 (Ed. K. C. Ludema
Am. Soc. Mech. Eng., New York, NY, 1985

FLASH TEMPERATURES DUE TO FRICTION AND JOULE HEAT AT ASPERITY CONTACTS

D. Kuhlmann-Wilsdorf
University of Virginia
Department of Materials Science
Charlottesville, Virginia

ABSTRACT

Approximate solutions, reliable within a few percent, have been obtained for the theoretical flash temperatures at circular and elliptical contact spots between two homogeneous materials when heat is evolved at the (assumed mathematically flat and uncontaminated) interface at a uniform rate, either independent of velocity as in the case of Joule heat, or in proportion with the relative speed, i.e. as is the case for friction heat. The parameters appearing in the corresponding equations have been expressed in terms of known materials properties plus the number of contact spots and their axis ratio. The accuracy with which the flash temperatures can be known in practice is limited by uncertainty regarding those parameters, and the idealizations embodied in the model. Those theoretical uncertainties are probably no larger than the actual momentary fluctuations of the conditions at the contact spots.

LIST OF SYMBOLS

a	Characteristic dimension of current-carrying circular contact spots, i.e. a-spots
$_EA$	Total load-bearing area in the elastic case
$_PA=P/H_S$	Total Load Bearing area in the plastic case
A	Length of load-bearing contact spot in direction of motion
B	Breadth of load-bearing contact spot at right angles to A
c	Specific heat
d	Mechanical density
$e=A/B$	Axis ratio of elliptical load-bearing contact spot
E	Young's modulus
$f(Z,S)$	Describes the velocity and shape dependence of the flash temperature: $\Delta T_e = \Delta T_o f(Z,S)$
$F=\pi AB/4$	Area of load-bearing contact spot
H_S	Mechanical hardness of the softer side
I	Total current flowing between the two sides
N	Number of contact spots
P	"Load", i.e. normal force between the two sides
q	Heat input per unit time and contact spot area
Q	Rate of total heat generation
$r=\sqrt{F/\pi}$	Characteristic dimension of load-bearing contact spot
r_2	Radius of curvature of asperity making elastic contact with the substrate
R	Electrical resistance
S	Shape factor
S_o	Shape factor at zero velocity and up to $v_r=1$
T	Temperature
$\bar{T}$	Average temperature of contact spot above ambient
$T_o=qr/\lambda_1$	Reference temperature (circular spot at v=0 when the asperity is thermally insulating)
v	Sliding velocity of the asperity (side 2) over the substrate (side 1)
v_o	Characteristic velocity ($v_o=\chi_1/r$ or $v_o=\chi_1/a$, respectively)
$v_r=v/v_o$	Relative velocity between the two sides
Z	Function needed for computing the velocity dependence of the flash temperature
Z_o	Z for circular contact spots

$\kappa=\lambda/dc$ Thermal diffusivitiy

Heat condutivity

$\lambda_r=\lambda_2/\lambda_1$ Heat conductivity of the asperity side relative to the substrate

μ Coefficient of friction

ν Poisson's ratio

ϱ Electrical resistivity of the sliding materials

σ_f Film resistivity (electrical resistance of unit area of film)

Subscripts

a Pertaining to a-spots

c Pertaining to constriction resistance

e Pertaining to elliptical contact spots

E Pertaining to elastically deformedcontact spots

f Pertaining to electrical film resistance

F Pertaining to friction

J Pertaining to Joule heat

P Pertaining to plastically deformed contact spots

r Standing for "relative"

T Pertaining to current conductionviaelectron tunneling through surface films

1 Pertaining to side 1 of the sliding pair, the substrate

2 Pertaining to side 2 of the sliding pair, the asperity

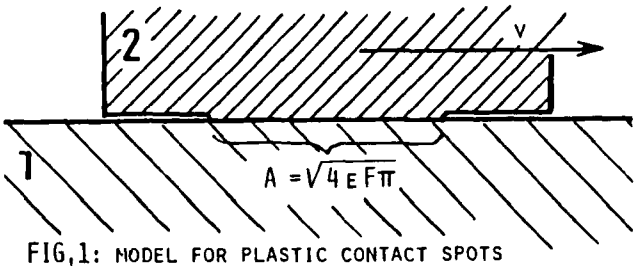

FIG.1: MODEL FOR PLASTIC CONTACT SPOTS

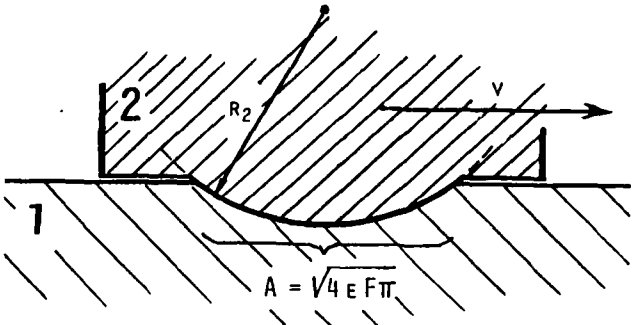

FIG.2: MODEL FOR ELASTIC CONTACT SPOTS

FUNDAMENTAL RELATIONSHIPS

In a previous set of two papers [1] the following expression was derived for the flash temperature at an elliptical contact spot between two semi-infinite materials as shown in Fig. 1, based on the fundamental earlier work by Blok [2] and Jaeger [3,4].

$$\Delta T_e = qr/\{\lambda_1/[z_o(v_r)S(v_r)] + \lambda_2/S_o\} \quad (1)$$

where

$$v_r = v/v_o = v/(\kappa_1/r) \quad (2)$$

with subscripts 1 and 2 referring to the two sides as indicated in Fig.1 and in the list of symbols, where also the other symbols are explained.

The function z_o was numerically known from ref.3, but no analytical expression for it, except that for very low speeds it becomes unity, and at very high speeds approximates $(9/8)/\sqrt{v_r}$.

By means of a simple model, in which the diffusion distances of the heat energy are considered, the following approximations were derived and found to compare to Jaeger's numerical values within a few percent over the whole range of speeds [1]:

$$z_o(v_r \leq 2) = 1/(1 + v_r/3) \quad (3a)$$

and

$$z_o(v_r \geq 2) = (9/8)/(\sqrt{v_r} + 1/\sqrt{8}). \quad (3b)$$

Using the same approach the shape factor, S, was found to be approximately given by

$$S(v_r \leq 1) = S_o = (4/3)/[(1 + e^{3/4}/3)(1 + 1/3e^{3/4}]^{1/2} \quad (4a)$$

and

$$S(v_r \geq 1) = (e^{1/4} + e^{1/4}/\sqrt{8v_r})/(1 + e^{3/4}/\sqrt{8v_r}). \quad (4b)$$

In order to employ eqs.1 to 4 above for the evaluation of flash temperatures in actual cases, one must know the various parameters appearing therein. Except for q and r, these are obvious and will ordinarily be known within reasonably narrow limits. The discussion therefore now turns to the determination of q and r. In this, one may treat different additive contributions to the total heat evolution separately, at least to a first-order approximation, since the excess of the flash temperature above ambient is simply proportional to q, as seen. Correspondingly, we may write

$$q = q_F + q_J \quad (5)$$

where q_F and q_J signify the heat evolution due to friction and joule heat, respectively. However, since q is the rate of heat evolution per unit area of contact spot, one must generally not only know how much total heat is evolved in order to know q, but also the size of the spots, i.e. r or a. As we shall see, this causes some complications.

EVALUATION OF r AND a, THE CHARACTERISTIC SPOT SIZES

(i) The Dimension $_pr$ of Plastic Contact Spots

When the load-bearing contact spots are plastically deformed, the average normal pressure over the whole area of real contact, independent of the number and shape of participating contact spots, approximates H_S, the (Meyer) hardness of the softer of the two sides, be it the asperity or substrate side.

In that case, then, the total load between the two sides, P, is supported by the total area $_pA$ of the plastically deformed load-bearing contact spots, say, N in number, so that

$$_pA = P/H_S = N\pi\, {}_pr^2 \tag{6a}$$

or

$$_pr = \sqrt{P/\pi N H_S} \,. \tag{6b}$$

(ii) The Dimension $_Er$ of Elastic Contact Spots

In the majority of cases, when wear occurs, the contact spots are plastic, in accordance with the above derivation. However, at very light loads, or when two very hard or brittle materials contact, or else if repeated contact is made at the same spots, the behavior can be elastic. In that case, following R. Holm [5] and again for N contact spots under total load P,

$$_Er = \{(3P/4N)[(1-\nu_1^2)/E_1 + (1-\nu_2^2)/E_2]\, r_2\}^{1/3} \tag{7a}$$

where ν stands for Poisson's ratio, E for Young's modulus, and r_2 is the radius of curvature of the asperity.

On the assumption that neither ν_1 nor ν_2 differ too much from 1/3, and with $1/E_1 + 1/E_2 = 1/E_{ave}$ this somewhat cumbersome expression becomes

$$_Er = (2Pr_2/3NE_{ave})^{1/3} \,, \tag{7b}$$

and correspondingly the total load-bearing area in the elastic case is approximately given by

$$_EA = N\pi\, {}_Er^2 = 2.4\ (NP^2 r_2^2/E_{ave}^2)^{1/3} \,. \tag{7c}$$

Strictly speaking, the model of Fig.1 on which eqs. 1 to 4 are based is incompatible with an elastic contact spot caused by a spherical asperity meeting a half-plane, described by the Hertzian eq.7. However, the heat flow between the two sides is negligibly affected if Fig.2 is substituted for Fig. 1, as implied by eq.7. The error resulting therefrom is certainly smaller than that due to any of the other causes, unless r_2 is comparable in magnitude to A.

(iii) The Dimensions of Current Carrying Contact Spots.

The areas of current-carrying contact spots, generally referred to as "a-spots" [5] do not necessarily coincide with load-bearing areas. Overwhelmingly (but as we shall see not exclusively) current passes only where load-bearing contact is established. Yet on account of uneven coverage by surface films of varied nature, enormous local fluctuations of contact resistance and, hence, of current density can exist, such as at cracks in oxide layers. Correspondingly, no blanket statements as to the values of a can be made, but each case must be considered individually. Only in the presence of very uniform surface coverage with either a conducting film or a "tunneling film", i.e. a film thin enough to permit electron tunneling, can general equations be applied.

If either type of uniform film is present, and the contact spots are plastically deformed, the associated value of the a-spot radius is simply

$$_pa = {}_pr \,, \tag{8}$$

and similarly for comparatively large elastic contact spots

$$_Ea = {}_Er \,. \tag{9}$$

Finally, it is possible that the contact spots are so small relative to the radius of curvature of the asperity (i.e. for $A \ll r_2$ in Fig.2) that the tunneling current about the periphery of the load-bearing spots becomes significant. Namely, electrons tunnel not only through very thin films but similarly through any narrow gap between two materials, and thus also through the annular wedge-shaped gap about the periphery of the contact spots. This effect may be enhanced by elastic deformation through adhesive forces acting through the same gap, leading to a slight expansion of the contacting area. As a result, current will flow through a somewhat larger area than necessary for elastic load-bearing, but the corresponding increase of a above r is negligible, indeed undiscoverable, except for extremely small elastic contact spots.

In previous papers evidence for peripheral tunneling has been discovered and the corresponding theoretical considerations have been presented [6-10]. The appropriate value of a is [5]

$$_Ta = ({}_Er^2 + 2sr_2)^{1/2} \tag{10}$$

with s the gap width (before deformation through adhesive forces, if any) through which tunneling takes place. In the cases studied in refs. 6 to 8, the parameter s was found to be near 5 angstroms.

EVALUATION OF q_{pr} DUE TO FRICTIONAL HEAT

When two materials slide past each other with velocity v under the load P with a friction coefficient μ, heat is developed at the rate

$$Q_F = \mu P v \ . \tag{11}$$

Since this heat evolution takes place at the contact spots we find, for the subscript i standing for either P or E, i.e. the plastic or elastic case,

$$_iq_F = Q_F/N\pi\ _ir^2 \tag{12}$$

and

$$_iq_F\ _ir = Pv/N\pi\ _ir \ . \tag{13}$$

For the plastic case, thus

$$_pq_F\ _pr = \mu v\sqrt{PH_s/N\pi}\ , \tag{14}$$

and for the elastic case

$$_Eq_F\ _Er = 0.364\,\mu v(P^2E_{ave}/r_2N^2)^{1/3} \ . \tag{15}$$

EVALUATION OF q_Jr DUE TO JOULE HEATING

(i) Film Resistance Heating

At or very near the interface Joule heat is developed from two causes. One of these is the electrical resistance of the ubiquitous surface films, and be they only monomolecular absorption layers. If these are not present, the two sides weld together, and the theory breaks down in any event on account of "galling" or "seizing".

Designating the specific film resistance by the symbol σ_f, the total Joule heat generated is

$$_fQ_J = I^2R_f = I^2\sigma_f/N_a\pi\ _ia^2 \tag{16}$$

where $_ia$ can stand for $_pa$, $_Ea$ or $_Ta$, as the case may be, and the subscript a at N_a shall draw attention to the fact that the number of a-spots can be larger or smaller than the number of load-bearing spots, and this by factors as large as ten either way, and perhaps larger yet.

Correspondingly,,

$$_fq_J = I^2\sigma_f/(N_a\pi\ _ia^2)^2 \tag{17}$$

and

$$_fq_J\ _ia = I^2\sigma_f/N_a^2\pi^2\ \ _ia^3 \ . \tag{18}$$

For the particular case that a uniform film exists overthewhole surface, we have N_a=N with $_pa = {}_pr$ for plastic contact spots and $_Ea = {}_Er$ for elastic spots in accordance with equations 6a and b. If so, we have

$$_pf q_J\ _pr = I^2\sigma_f(H_s^3/P^3\pi N)^{1/2} \ . \tag{19}$$

Similarly, when with entirely uniform surface coverage the contact spots are elastic, so that eq. 7 may be used, one obtains approximately

$$_Ef q_J\ _Er = 0.153\ I^2\sigma_f E_{ave}/PNr_2 \ . \tag{20}$$

(ii) Constriction Resistance Heating

The second contribution to Joule heat at or near the interface is due to the constriction resistance. This arises because all of the current has to pass through the a-spots and thus the current flow lines are strongly constricted at the interface. The effect is much as if the two solids were connected by N_a wires of the same diameter as the a-spots and a length comparable to their radius, but unlike the film resistance it depends on the shape of the a-spots. Approximately, the constriction resistance of N_a elliptical a-spots with axis ratio e = A/B and area $\pi\ _ia^2$ each is, according to eqs.4.23 and 4.27 of ref.5,

$$_iR_c = (\rho_1+\rho_2)[\ln(2\sqrt{e})/\sqrt{e}]/N_a\pi\ _ia \tag{21a}$$

where once again the subscript i can signify P, E or T, while ρ is the electrical resistivity of the sliding materials. However, for $e \leq 1.4$

$$_iR_c = (\rho_1+\rho_2)/4N_a\pi\ _ia \tag{21b}$$

is abetter approximation which indeed is exact for e=1. Correspondingly, it is

$$_ic Q_J = I^2\ _iR_c \tag{22}$$

and

$$_ic q_J \equiv {}_ic Q_J/N_a\pi\ _ia^2 \tag{23}$$

and

$$_ic q_J\ _ia = I^2(\rho_1+\rho_2)[\ln(2\sqrt{e})/\sqrt{e}]/(N_a\pi\ _ia)^2 \ . \tag{24}$$

For the case of unifcrm surface coverage with a conducting film or a tunneling film we thus obtain, for plastic contact spots,

$$_pc q_J\ _pr = I^2(\rho_1+\rho_2)[\ln(2\sqrt{e})/\sqrt{e}](H_s/P\pi N) \ . \tag{25}$$

Similarly, for elastic contact spots obtain

$$_Ec q_J\ _Er = 0.133\ I^2(\rho_1+\rho_2)[\ln(2\sqrt{e})/\sqrt{e}](E_{ave}/N^2Pr_2)^{2/3} \tag{26}$$

We shall not specifically discuss the case of reduction of joule heat through peripheral tunneling since this is of very specialized interest only, is ordinarily a minor effect, and has been discussed in refs. 8 to 10. Therefore, in summary of this section, then, the heat flow density due to electric currents is $_iq_J = {}_if q_J + {}_ic q_J$.

SUMMARY OF EQUATIONS

We may rewrite eq.1 as

$$\Delta T_e = \Delta T_o f(Z,S) \tag{27a}$$

where

$$\Delta T_o = qr/\lambda_1 = q\sqrt{F/\pi}/\lambda_1 \tag{27b}$$

and

$$f(Z,S) = (1/Z_o(v_r)S(v_r) + \lambda_r/S_o)^{-1}. \tag{27c}$$

In this general formulation, ΔT_e is the sum of all contributions to the flash temperature which simply superimpose (at least to a first approximation) as q is the sum of all contributions. Thus

$$\Delta T_e = \Delta T_{eF} + \Delta T_{eJ} \tag{27d}$$

and

$$q = q_F + q_J = q_F + {}_f q_J + {}_c q_J \tag{27e}$$

as discussed in the previous section, while

$$\lambda_r = \lambda_2/\lambda_1 \tag{27f}$$

and $v_r = v/v_o = v/(\kappa_1/r)$ in accordance with eq.2. As before, r is the characteristic dimension of the contact spot, namely

$$r = \sqrt{F/\pi}\ , \tag{27g}$$

of which the specific values ${}_pr$, ${}_Er$, ${}_pa$, ${}_Ea$ and ${}_Ta$ were given above in eqs.6-10.

As we saw, it is not generally possible to give values for q_J except when the surface film has uniform electrical resistance everywhere. For that particular case, based on eqs.13, 18 and 24 obtain

$$\Delta T_e = [f(Z,S)/\lambda_1]\{\mu Pv/(N\pi\,{}_ir) + I^2\sigma_f/(N^2\pi^2\,{}_ir^3) + I^2(\rho_1+\rho_2)[\ln(2\sqrt{e})/\sqrt{e}]/(N\pi\,{}_ir)^2\} \tag{28}$$

where ${}_ir$ is either ${}_pr$ or ${}_Er$.

Hence from eqs 14, 19 and 25

$${}_p\Delta T_e = [f(Z,S)/\lambda_1]\{\mu v\sqrt{PH_B/N\pi} + I^2\sigma_f(H_B^3/P^3\pi N)^{1/2} + I^2(\rho_1+\rho_2)[\ln(2\sqrt{e})/\sqrt{e}](H_B/P\pi N)\} \tag{29}$$

and from eqs 15, 20 and 26

$${}_E\Delta T_e = [f(Z,S)/\lambda_1]\{0.364\,\mu v(P^2E_{ave}/r_2N^2)^{1/3} + 0.153\,I^2\sigma_f E_{ave}/PNr_2 + 0.133\,I^2(\rho_1+\rho_2)[\ln(2\sqrt{e})/\sqrt{e}](E_{ave}/N^2Pr_2)^{2/3}\} \tag{30}$$

while

$${}_pv_r = v\sqrt{P/N\pi H_B}\,/\kappa_1 \tag{31}$$

and

$${}_Ev_r = v(2Pr_2/3NE_{ave})^{1/3}/\kappa_1\ . \tag{32}$$

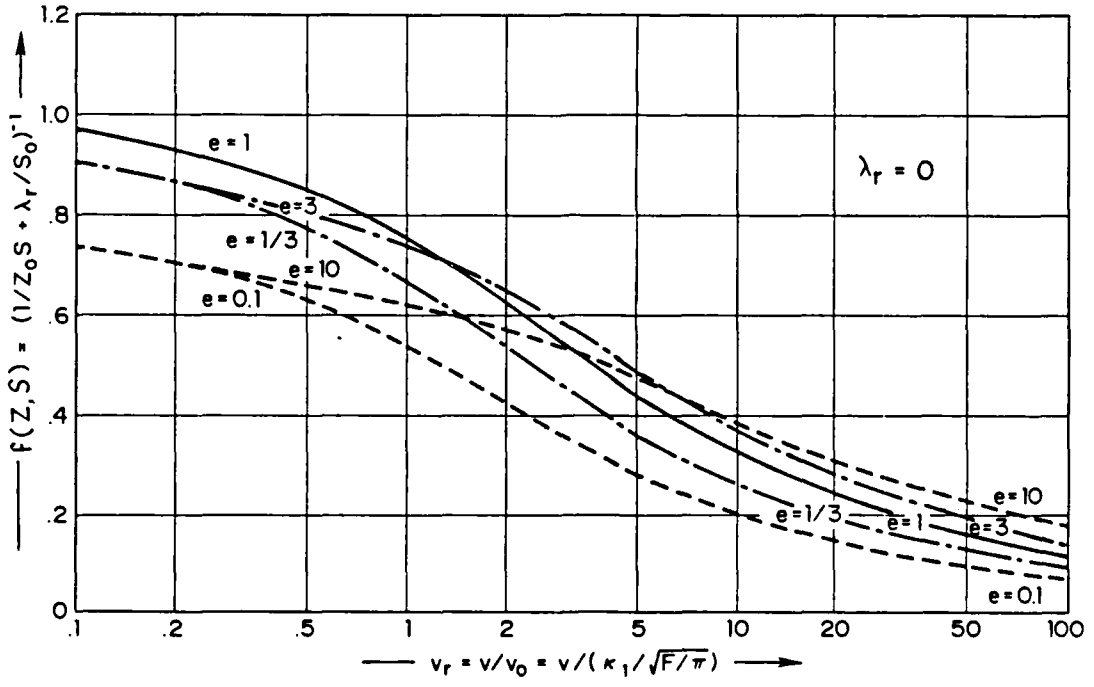

FIG.3

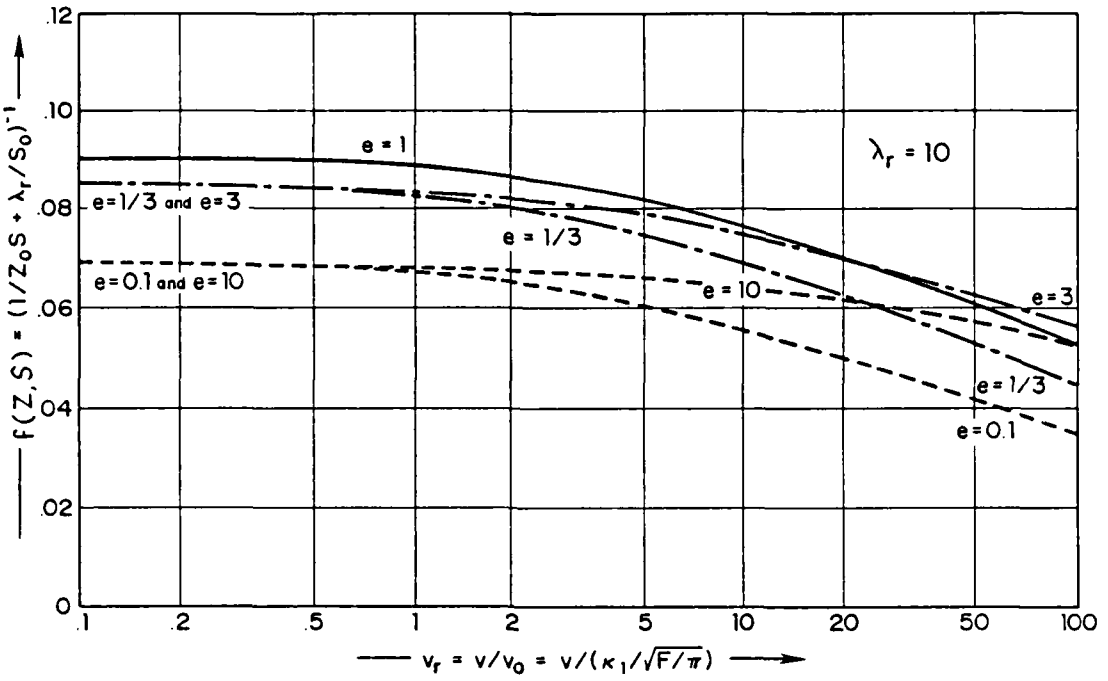

FIG.4

DISCUSSION

$T_o = qr/\lambda_1$ is the flash temperature of a circular contact spot at rest, comprising a thermally insulating asperity side, but having the same area, located on the same substrate, and experiencing the same rate of heat input, as the contact spot under consideration. The function f(Z,S) corrects this basic flash temperature in accordance with the actually existing modifications due to the facts that the actual contact spot is generally (i) in motion, (ii) elliptical, and (iii) that the asperity side is ordinarily not a thermal insulator so that not all of the heat flows into the substrate (although the fraction that flows in that direction increases steadily with increasing speed because more and more of the heat is expended in warming up a surface layer of the fresh track on the substrate).

All three of the named effects diminish the flash temperature, so that ΔT_o is the highest flash temperature that can be generated at a spot of the area $F = \pi r^2$ situated on the given substrate material and heated by heat input q per unit area. Correspondingly, the function f(Z,S), shown for $\lambda_r = 0$ and for $\lambda_r = 10$ in Figs.3 and 4, is never larger than unity, and steadily decreases with rising speed and heat conductivity of the asperity side.

In regard to ellipticity f(Z,S) is not symmetrical with respect to e = A/B. This is for the reason that a contact spot stretched out in the direction of motion leaves behind a narrower warmed track on the substrate than a spot of same area which is wide at right angles to the direction of motion; and thus the flash temperature of the former is higher than of the latter.

While evidently none of the derivations or expressions given above are inherently difficult, their practical application is still cumbersome, albeit by far more managable than in the few previously available treatments. Moreover, the functional dependence of the flash temperature on velocity was known only imperfectly and its shape dependence even less, although one should hasten to add that Holm [5] has by a different route arrived at another, and perhaps more accurate, method of evaluating flash temperatures under a wide range of circumstances.

The variations in which the equations can be written are manifold, and in somewhat different formulations they have been assembled in form of a table in refs. [8] and [10], where also some numerical examples for the flash temperature are given for the case of circular a-spots.

One has no reason to be surprised that the equations are so involved: The number of physical parameters and variables which in actuality determine the flash temperature is considerable, and somehow the equations have to accommodate that fact.

We have already pointed out at the beginning, that the reliability of the obtained numerical values can be no better than the input parameters plus the approximations inherent in the model. Yet, results

that have variously been computed for particular cases (8,10) give the impression of being gratifyingly close to fact, wherein as a rule of thumb N = 10 is a good choice unless one knows the number of contact spots more reliably from some other source.

ACKNOWLEDGEMETS

The financial support of this research through the Materials Division (Tribology) of the Office of Naval Research, Arlington, VA, is gratefully acknowledged.

REFERENCES

1) D. Ruhlmann-Wilsdorf, Wear, submitted for publ.
2) H. Blok, Proc. General Disc. on Lubrication and Lubricants, Inst. Mech. Eng., 2 (1937) 14.
3) J. C. Jaeger, J. Proc. Roy. Soc. N. S. W. 56 (1942) 203.
4) H. S. Carslaw and J. C. Jaeger, The Conduction of Heat in Solids, Oxford Univ. Press, London.
5) R. Holm, Electric Contacts (Springer-Verlag, Berlin/ Heidelberg, 4th Ed. 1967).
6) C. M. Adkins and D. Ruhlmann-Wilsdorf, "Electrical Contacts - 1979" (Ill. Inst. Techn., Chicago, IL, 1979), p.171.
7) C. M. Adkins and D. Ruhlmann-Wilsdorf, "Electrical Contacts - 1980" (Ill. Inst. Techn., Chicago, IL, 1980), p.67.
8) D. Ruhlmann-Wilsdorf, "Electrical Contacts - 1983" (Ill. Inst. Techn., Chicago, IL, 1983), p.21.
9) D. Ruhlmann-Wilsdorf, Proc. 1983 Meetg. Electrochem. Soc., Washington, DC, p.407.
10) D. Ruhlmann-Wilsdorf, Proc. 2nd. Symp. on Electromagnetic Launch Technology (Boston, MA, Oct. 1984) p.133; IEEE Trans. on Magnetics, Vol. MAG-20, #2 (1984) p.340.

END

FILMED

6-85

DTIC